Exp Brain Res (1991) 86:271–292

Experimental Brain Research

Direct and indirect retinal input into degenerated dorsal lateral geniculate nucleus after striate cortical removal in monkey: implications for residual vision

Z.F. Kisvárday[1,2,3]*, A. Cowey[1], P. Stoerig[4], and P. Somogyi[2,3]

[1] Department of Experimental Psychology, Oxford University, South Parks Road Oxford, OX1 3UD, UK
[2] MRC Anatomical Neuropharmacology Unit, South Parks Road, Oxford OX1 3QT, UK
[3] United Research Organization of the Hungarian Academy of Sciences and Semmelweis University Medical School, Tűzoltó u. 58, H–1094 Budapest, Hungary
[4] Institute of Medical Psychology, Ludwig-Maximilians University, Goethestrasse 31, W–8000 Munich 2, Federal Republic of Germany

Received February 7, 1991 / Accepted May 7, 1991

Summary. We removed the striate cortex of one cerebral hemisphere in a macaque monkey, causing almost total retrograde degeneration of the corresponding dorsal lateral geniculate nucleus (dLGN) and extensive transneuronal degeneration of ganglion cells in the corresponding hemi-retina of each eye. The rare surviving geniculate projection neurons were retrogradely labelled by horseradish peroxidase (HRP) from extra-striate cortex and retinogeniculate terminals were labelled by an intraocular injection of HRP. Retinal terminals in the degenerated dLGN made synaptic contact exclusively with the dendrites of interneurons immunopositive for γ-aminobutyric acid (GABA) in both parvocellular and magnocellular regions of dLGN. As well as being postsynaptic to retinal terminals these vescicle-containing dendrites were pre- and postsynaptic to other similar dendrites, and presynaptic to relay cells. Surviving labelled projection neurons received retinal input indirectly, via both the GABA-immunopositive interneurons and GABA-immunonegative terminals characteristic of those from the superior colliculus. In the degenerated, as opposed to the normal dLGN, about 20% of retinal terminals were GABA-immunopositive and GABA-immunoreactivity was prominently elevated in the ganglion and amacrine cell layers of the degenerated half of the retina. The optic nerve also contained numerous GABA-immunopositive axons but very few such axons were found in a normal optic nerve processed in identical manner. The surviving pathways from the retina must underlie the visual abilities that survive striate cortical removal in monkeys and human patients and may involve the degenerated dLGN as well as the mid-brain.

Key words: Visual cortex – Retina – Thalamus – Blindsight – GABA

Introduction

When part of the striate cortex (area 17, or V1) is destroyed in primates about 99% of the projection neurons in the topographically corresponding part of the dorsal lateral geniculate nucleus (dLGN) degenerate within 12 weeks (Mihailovic et al. 1971). The few that survive, apparently permanently (van Buren 1963; Yukie and Iwai 1981; Dineen et al. 1982; Cowey and Stoerig 1989), are present in both the parvo- and magno-cellular divisions of the nucleus, and within as well as between the laminae. They can be retrogradely labelled by HRP injected into cortical visual areas V2 and V4 and presumably survive because of this extrastriate projection (Yukie and Iwai 1981; Fries 1981; Hendrickson and Dineen 1982; Bullier and Kennedy 1983; Cowey and Stoerig 1989). It has been suggested (Hendrickson and Dineen 1982; Dineen et al. 1982; Cowey and Stoerig 1989) that these cells may contribute to the residual abilities that remain within the field defects caused by destruction of part of striate cortex. These abilities are extensive and include detection and localization of stimuli as well as discrimination based on orientation, direction, motion, form, and wavelength (reviewed by Weiskrantz 1989).

Unlike the direct or indirect retinal inputs to the retrogradely degenerated dLGN, those to the normal dLGN in primates are well known. The two mag-

* Present address: Ruhr-Universität Bochum, Department of Neurophysiology, Universitätsstrasse 150, W–4630 Bochum 1, Federal Republic of Germany

Offprint requests to: A. Cowey (address see above)

nocellular layers in the dLGN are the target zone of the primate alpha (Pα) ganglion cells (Perry et al. 1984; Leventhal et al. 1981). Functionally, they have broad-band characteristics, with high sensitivity to contrast and temporal modulation, and are candidates for transmitting signals for motion perception, stereopsis, and form from shading (see Livingstone and Hubel 1988, for review). The primate beta (Pβ) ganglion cells project to the four parvocellular layers (Perry et al. 1984). Like their geniculate targets they are predominantly colour opponent, with high spatial and comparatively low temporal resolution (see Shapley and Perry 1986, for review), suggesting their involvement in form and colour vision (Livingstone and Hubel 1988). Selective destruction of Pβ ganglion cells or of the parvocellular portion of the dLGN produces deficits in spatial resolution and colour discrimination in monkeys (Merigan and Eskin 1986; Schiller et al. 1990). As no other group of cells receiving direct retinal terminals is known to carry colour-opponent signals, they are particularly interesting in view of the evidence of colour opponent processing in the "blind" field defects of patients (Stoerig and Cowey 1989b, 1990) and in monkeys in which all the striate cortex has been removed (Schilder et al. 1972; Keating 1979). Finally, the primate gamma (Pγ) retinal ganglion cells are morphologically heterogeneous and project to the superior colliculus, the pretectum (Perry and Cowey 1984; Leventhal et al. 1981), and perhaps the interlaminar layers of the dLGN (Fitzpatrick et al. 1983; Weber et al. 1983). The admittedly small sample that has been examined was neurophysiologically heterogenous, but sensitivity to moving stimuli was prominent (de Monasterio 1978b), and colour-opponency was absent (Schiller and Malpeli 1977b). Cells in their target zone in the superior colliculus project to the dLGN, particularly to the S-layers and to the interlaminar zones, including the intercalated layer between the parvo- and magnocellular divisions (reviewed by Huerta and Harting 1984).

The role of this tecto-geniculate pathway is mysterious but must be considered in view of the evidence that at least some aspects of residual vision following striate cortical damage in monkeys are abolished by subsequent damage to the superior colliculus (Mohler and Wurtz 1977), as are the selective responses to visual movement of neurons in visual area MT that survive removal of the striate cortex (Rodman et al. 1989). Although there appears to be no direct projection from the dLGN to area MT (Benevento and Standage 1982) Schiller et al. (1990) showed that monkeys could not make saccades to targets in field defects caused by destruction of all layers of the dLGN, implying that other collicular projections to extrastriate cortical areas either do not suffice to sustain them or are functionally disrupted by the geniculate lesion.

As yet, there is no evidence that the geniculate cells that survive destruction of striate cortex receive a direct or indirect retinal input and, therefore, that they could contribute to residual vision. The degenerated dLGN does receive retinal axons, as shown by light microscopic anterograde tracing methods (reviewed by Weller and Kaas 1989) but this alone does not indicate that they are in synaptic contact with surviving projection neurons, as implied by the results of Benevento and Yoshida (1981) who found no evidence of transynaptic labelling in extrastriate cortex following intra-ocular injections of tritiated amino acids. In an attempt to solve this problem, Dineen et al. (1982) used electron microscopic autoradiography to examine the ultrastructure within a degenerated dLGN. They showed that labelled terminals with the apparently unique, and therefore unambiguous, morphological characteristics of retino-geniculate terminals (Guillery and Colonnier 1970; Szentágothai 1973) were present in roughly equal densities in both parvo- and magno-cellular portions of the degenerated dLGN, and that they made contacts with neuronal elements. Unfortunately, no postsynaptic target was a large dendrite characteristic of a projection neuron, or a neuronal cell body. In an attempt to resolve this problem we studied a monkey in which the striate cortex of one hemisphere had been removed two and a half years previously. By injecting HRP into extra-striate cortex (chiefly V4) and into one eye, it was possible to examine identified retinal terminals (both labelled and unlabelled) in relation to neurons back-filled from cortex and to interneurons that were identified both on the basis of their morphological features (Hámori et al. 1974; Pasik et al. 1973; Szentágothai 1973) and the immunopositivity of their dendrites for GABA.

In addition, we examined the retina to confirm the retrograde transneuronal degeneration of the ganglion cell layer (Van Buren 1963; Cowey et al. 1989). We also looked for evidence of any unusual features of the metabolism of GABA in the degenerated hemiretina, where unusual characteristics of the pattern-evoked and Ganzfeld electroretinogram have been reported and attributed to functional changes in the ganglion and predominantly GABAergic amacrine cell populations (Stoerig and Zrenner 1989). Some of the results have been described in conference proceedings (Kisvárday et al. 1990).

Methods

Subject

The principal subject was a male feral *Macaca fascicularis*. He was about 5 years old at the beginning of this investigation, having taken part in visual discrimination experiments during the previous 2 years. We also used one eye from a normal female macaque that had been perfused in an identical manner immediately following a pharmacological experiment, and examined retinal sections from four other operated monkeys.

Surgery

The surgical procedures were performed under strict aseptic conditions with the aid of a stereo operating microscope. At the first operation the striate cortex of the left hemisphere was removed and the splenium of the corpus callosum was cut. The animal was sedated with 10 mg/kg i.m. of ketamine hydrochloride (Ketalar, Parke-Davis) then anaesthetised for the duration of the operation with sodium thiopentone i.v. (Intraval, May and Baker). The skin and fascia were cut along the midline and reflected laterally. A bone

flap, approximately 4 cm long by 3 cm wide, was turned across the midline and the dura opened to expose the dorsomedial shoulder of the left hemisphere for about 2 cm just rostral to the confluence of the intraparietal and lunate sulci. The medial surface of the hemisphere was gently retracted from the falx and the caudal 12 mm of the corpus callosum were severed with a 23 gauge blunt aspirator. The bone overlying the lateral surface of the left striate cortex was then removed and the dura was cut in order to reveal the underlying striate cortex. After cauterising any bridging vessels between the cortex and the dura the occipital lobe was severed 5 mm caudal to the lunate sulcus and removed. The remaining striate cortex just caudal to the lunate sulcus and in the rostral depths of the calcarine fissure were then removed by sub-pial suction. Any severed vessels were cauterised and the cut surface was covered in a thin layer of gel-foam. After sewing the dura, the midline bone flap was replaced and secured at its corners and the occipital opening was covered by the previously retracted temporal muscle. Fascia and skin were sewn, 300000 units of penicillin were given i.m. (Bicillin, Brocades) and the animal made a prompt recovery.

Thirty months later and using similar procedures the cortex of the prelunate gyrus, just rostral to the border of the previous lobectomy, was exposed and 18 fragments of HRP were implanted at the positions shown in Fig. 1. Each fragment was placed with fine forceps through a small cut in the pia and pushed laterally into the grey matter. The fragments whose entry points are shown alongside the superior temporal and lunate sulci were advanced into the bank of the sulcus. The HRP (Boehringer, type 1) was prepared by saturating a piece of gelfoam with a solution of 50% HRP in sterile water, allowing it to become almost dry in a sterile vessel, compressing it while still malleable, then cutting it into small fragments when totally dry. It was used while still fresh. After implanting the HRP the dura and overlying tissues were sewn. Anterograde tracer was then injected into the right eye as follows. A solution of 250 µl of L-(3,4(n)-3H)-proline, specific activity 50 Ci/mM (Radiochemicals Amersham) containing 250 mCi was reduced to 50 µl under a stream of nitrogen. HRP was added to make a 50% solution which was injected over a period of 10 minutes into the vitreous of the right eye using a sterile Hamilton syringe and while viewing the fundus ophthalmoscopically. After withdrawing the needle the limbus around the entry point was treated with 5% xylocaine ointment (Astra). Recovery was prompt and uneventful.

Histology

Three days later the animal was sedated and given a lethal dose of sodium pentobarbitone before being perfused through the heart with 600 ml of continuously oxygenated Tyrode's solution, followed by 4 litres of a fixative containing 1% glutaraldehyde (TAAB) and 1.5% paraformaldehyde (TAAB) in 0.1 M phosphate buffer (PB), pH 7.4. The eyes were removed following fixation for subsequent sectioning. While still in place the brain was cut into three blocks by two coronal cuts in the stereotaxic frontal plane, through the optic chiasma rostrally and behind the dLGN caudally. The posterior block, through the lesion, was photographed and placed for 3 days in a solution of 30% sucrose dissolved in PB before being sectioned in the coronal plane at 50 µm on a freezing microtome. Every fifth section was reacted for HRP using the protocol of Perry and Linden (1982) and counterstained with cresyl fast violet acetate. These sections were used to reconstruct the site of the lesion and the position of the HRP (Fig. 1). The central block, containing the geniculates, was trimmed until each dLGN was contained within a block measuring 10 by 10 mm in cross section.

Tissue processing

Blocks containing the dLGN were postfixed for 4 hours in the same fixative, and coronal sections (70–80 µm) were cut on a vibratome and collected in series in 0.1 PB. Every fourth section was mounted on slides and stained for Nissl substance. Histochemical detection of HRP transported either retrogradely from the cortex or anterogradely from the eye was carried out using tetramethylbenzidine (TMB) as chromogen and ammonium-heptamolybdate (AHM) as stabilizing agent in 0.1 M PB at pH 6.0 (Olucha et al. 1985). For electron microscopy the TMB–AHM reaction end-product was intensified by incubating the sections in 0.05% 3,3′-diaminobenzidine in the presence of 0.01% $CoCl_2$ dissolved in PB, pH 6.0. The sections were then rinsed in distilled water, treated with ice-cold osmium-tetroxide (1% in 0.1 M PB for 15 min), rinsed in PB, dehydrated, and mounted in epoxy resin (Durcupan ACM, Fluka) on slides.

Electron microscopy of the lateral geniculate nuclei

Thick sections containing retrogradely labelled neurons with dense accumulation of cortically injected HRP and corresponding tissue samples from the normal dLGN were removed from the slides and re-embedded into epoxy resin in plastic capsules. The laminar position of labelled cells was determined as follows: through the entire dLGN we had adjacent, or closely neighbouring, sections stained for Nissl substance or prepared for anterograde labelling by autoradiography and by HRP histochemistry, together with a fourth series reacted for GABA. The laminar boundaries were drawn from all types of section. One drawn series is shown in Fig. 2, and reveals a reassuring coincidence in the boundaries revealed by the different techniques. It was therefore possible to estimate the laminar position of the cells selected for electron microscopic analysis in the intervening osmium treated sections. Their positions are shown in Fig. 4. The soma and some of the dendrites of these chosen cells were sectioned in series, through a depth of about 15–50 µm, and the sections were mounted on formvar coated single slot grids. Samples from the series were examined, leading to the identification of about 250 synaptic contacts on the retrogradely labelled neurons. The sections were contrasted with lead-citrate.

Postembedding GABA-immunostaining on semithin sections

To compare the distribution of GABA-immunopositive cells between the normal and the degenerated dLGN, sections of 0.5 µm thickness were cut from each side at corresponding levels and mounted onto chrome-alum gelatin coated slides. Immunocytochemistry for GABA was carried out as reported earlier (Somogyi 1988), using a previously characterized antiserum to GABA raised in rabbit (Hodgson et al. 1985; code No. 9) and the unlabelled antibody peroxidase-antiperoxidase method (Sternberger et al. 1970). Peroxidase was reacted with 3,3′-diaminobenzidine tetrahydrochloride (DAB) as chromogen (0.05%) and H_2O_2 as substrate (0.01%) in 50 mM tris buffer.

Postembedding GABA-immunostaining on ultrathin sections

To establish the chemical characteristics of synaptic elements in both dLGNs, some of the ultrathin sections were reacted with an antiserum to GABA using the colloidal gold method (Somogyi 1988). Briefly, sections were treated with 1% periodic acid and 1% sodium periodate for 10 min to etch the resin and remove osmium. After washing the sections thoroughly in distilled water and 50 mM trisbuffered saline (TBS, pH 7.4) they were placed on droplets of 1% aqueous solution of ovalbumin for 30 min. Rabbit anti-GABA serum (diluted 1:1000 in TBS containing 1% normal goat serum) was applied for 2 hours followed by washes in TBS for 2 × 5 min, and in 0.1% polyethylene glycol dissolved in 50 mM tris buffer (TB–PEG, pH 7.4) for 2 × 10 min. Thereafter the sections were incubated for 2 hours with goat anti-rabbit immunoglobulin cou-

pled to colloidal gold (15 nm, Bioclin) diluted 1:20 or 1:40 in TB–PEG, and rinsed thoroughly in distilled water. All incubation steps were carried out on droplets of Millipore filtered (size 0.22 μm) reagents. Following immunostaining, the sections were treated with osmium by exposing them to vapour for 1 min, stained with saturated uranyl-acetate for 20 min, and contrasted with lead citrate for 2 min.

Quantitative electron microscopy

Postsynaptic elements of labelled and unlabelled retinal terminals were quantitatively analysed from disparate areas of the normal and degenerated dLGN. Each retinal terminal, identified on the basis of electron microscopic criteria, that fell into the plane of the sections was taken into account and the postsynaptic elements were identified using ultrastructural characteristics and GABA-immunostaining. Retinal terminals were covered with varying density of gold particles following GABA-immunoreaction. Some of the terminals had gold densities similar to, or in excess of, that of adjacent F terminals which are believed to represent the neuronal elements responsible for GABAergic inhibition. In order to evaluate the GABA-immunoreactivity of retinal terminals the density of gold particles was calculated by measuring the area of the terminal and counting the gold particles using the Bioquant IV system and comparing the density with that over nearby GABAergic F terminals.

Retinal histology

Both eyes were removed after perfusion and placed in the same fixative at 4° C. After several weeks the left eye was processed as follows. The anterior chamber, lens, and much of the vitreous were removed. The eye cup was dehydrated in alcohol, cleared in toluene, and embedded in paraffin wax. Horizontal sections, parallel to the horizontal retinal meridian, were cut at 10 μm. After identifying the fovea, every 5th section through the central retina was mounted on a gelatinized slide, dewaxed, rehydrated, and stained for Nissl substance with cresyl fast violet acetate. Additional series were mounted and reacted for GABA using the same antiserum (dil. 1:4000) already described for semithin sections of dLGN. The primary antibody was visualised using HRP-conjugated sheep anti-rabbit IgG (Dako, diluted 1:50) and a light reaction with DAB as chromogen. The reaction product was silver-gold intensified as described earlier (Liposits et al. 1984). The sections were dehydrated, cleared and coverslipped in DPX without further processing.

Results

Cortical lesion and HRP transport

The striate cortex of the left hemisphere was completely removed apart from a small tag adjacent to the lunate sulcus at the midline, and corresponding to the representation of the vertical meridian at an eccentricity of 5–6 degrees. However, even this remnant was severed from the radiations beneath it and there was no sign of any neuronal island of spared cells in the dLGN at the appropriate retinotopic region at the ventro-medial edge of the nucleus about half way along its rostro-caudal axis. Histological detection of cortically implanted HRP pellets showed that the HRP covered the entire area of the prelunate gyrus and therefore the upper half of area V4, but may have involved area V2 in the vicinity of the spared ascending limb of the inferior occipital sulcus (Fig. 1).

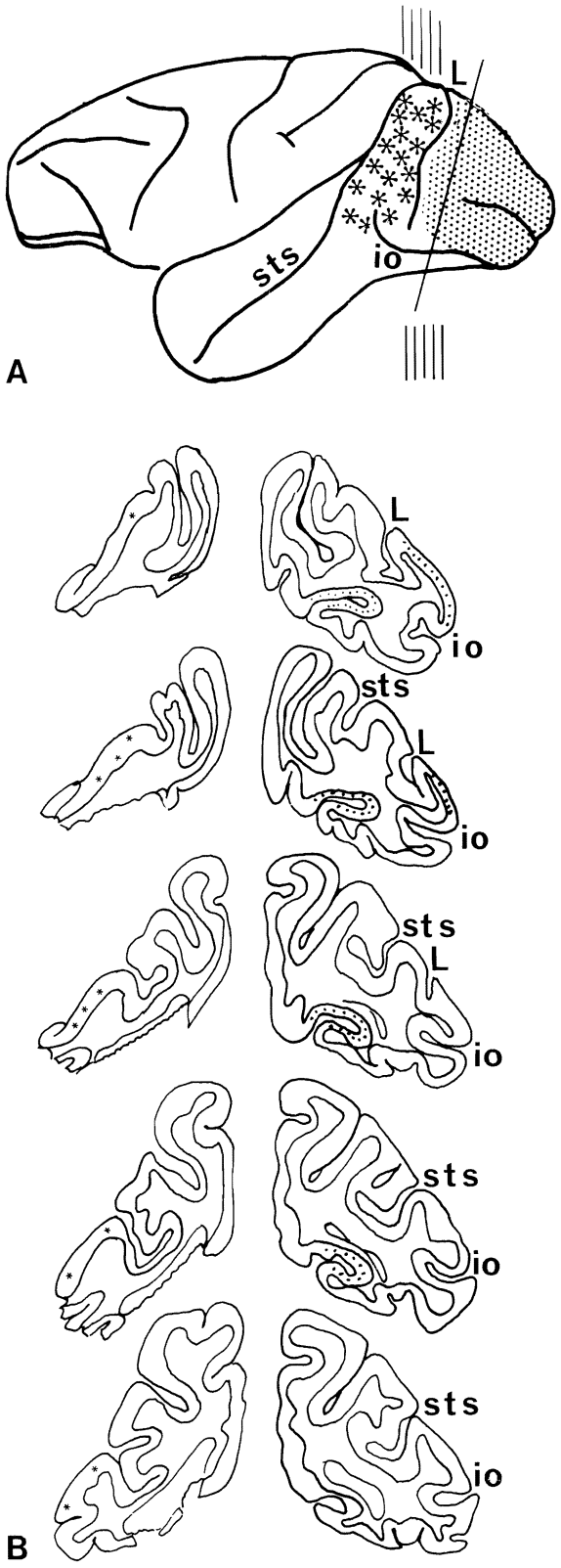

Fig. 1. A Outline of the left hemisphere showing the striate cortical ablation (shaded) and the position of HRP implants (asterisks) in the prelunate gyrus. The oblique line indicates the plane behind which all tissue was removed. **B** Drawings of frontal sections, from caudal to rostral, show some of the implant sites for HRP (asterisks) and that the striate cortex (dotted in right hemisphere) is missing on the left. l, lunate sulcus; io, inferior occipital sulcus; sts, superior temporal sulcus

Degeneration and HRP labelling in the left dLGN. The entire left dLGN degenerated and showed about 40% linear shrinkage with respect to its normal counterpart (Figs. 2, 3). In agreement with previous reports (Yukie and Iwai 1981; Cowey and Stoerig 1989) some neurons that survived the cortical ablation were retrogradely labelled with HRP from the extra-striate visual cortex. These labelled cells were found in the caudal two thirds of the left dLGN, with increasing density towards the most caudal part, where the fovea is represented. They were located mostly, but not exclusively, in the area occupied by the remnants of the parvocellular laminae and their interlaminar zones (e.g. Fig. 4).

HRP labelling from the eye. Anterograde transport of HRP injected into the right eye produced terminal labelling in both geniculate bodies. However, the labelling patterns were different in that in the normal dLGN labelled retinal terminals were equally distributed across the ipsilateral divisions of both magno- and parvocellular layers whereas in the left geniculate labelled fibres and terminals occurred more densely in the magno-cellular division (e.g. see Fig. 2). This confirms earlier reports (Dineen et al. 1982; Weller and Kaas 1989) that striate cortical ablation has a greater effect on the parvo-cellular than on the magno-cellular pathway. HRP-labelled retinal axons in the degenerated side often formed large diameter varicose segments, under the light microscope, which were never observed in the normal side.

Surviving neurons in the degenerated dLGN – light microscopic features

Two major types of neuron could be distinguished in Nissl-stained or in osmium-treated sections of the dLGN on the degenerated side. One type had a small soma (8–10 μm) and were scattered throughout the remnants of the

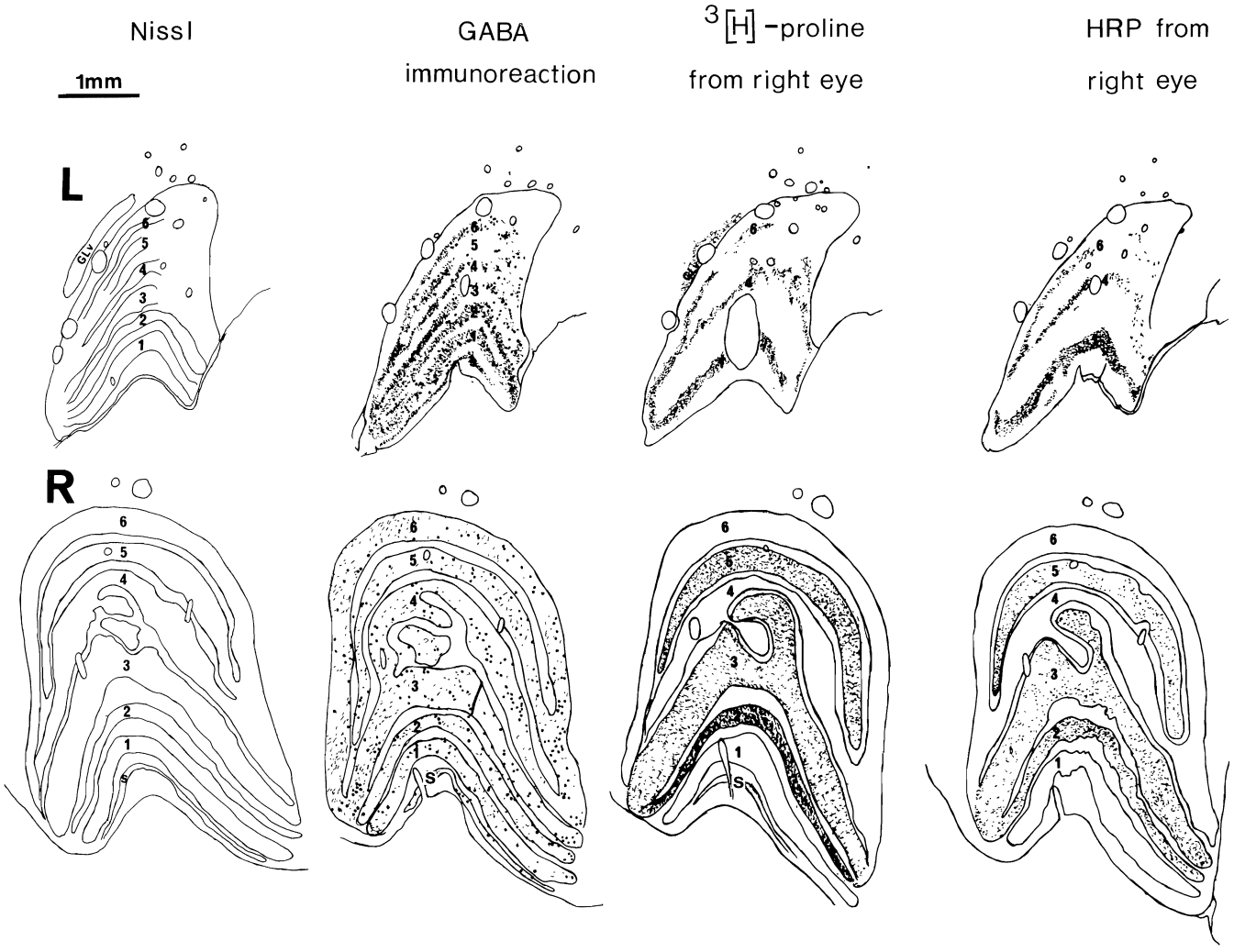

Fig. 2. Drawings of neighbouring sections from left (L) and right (R) dLGN, prepared with a drawing tube attached to a microscope. Slight differences in size with respect to the GABA-immunoreacted sections caused by shrinkage were adjusted by altering the magnification. The scale bar refers to both left and right. The large dots in the GABA-immunoreacted sections indicate the most prominent GABA-immunopositive neurons; less conspicuous ones were not marked. Intensities of labelling are comparable only within the same procedure. The layers are numbered from 1 to 6 in the conventional way. s = S layers, in the left dLGN only visible in the GABA-immunoreacted sections

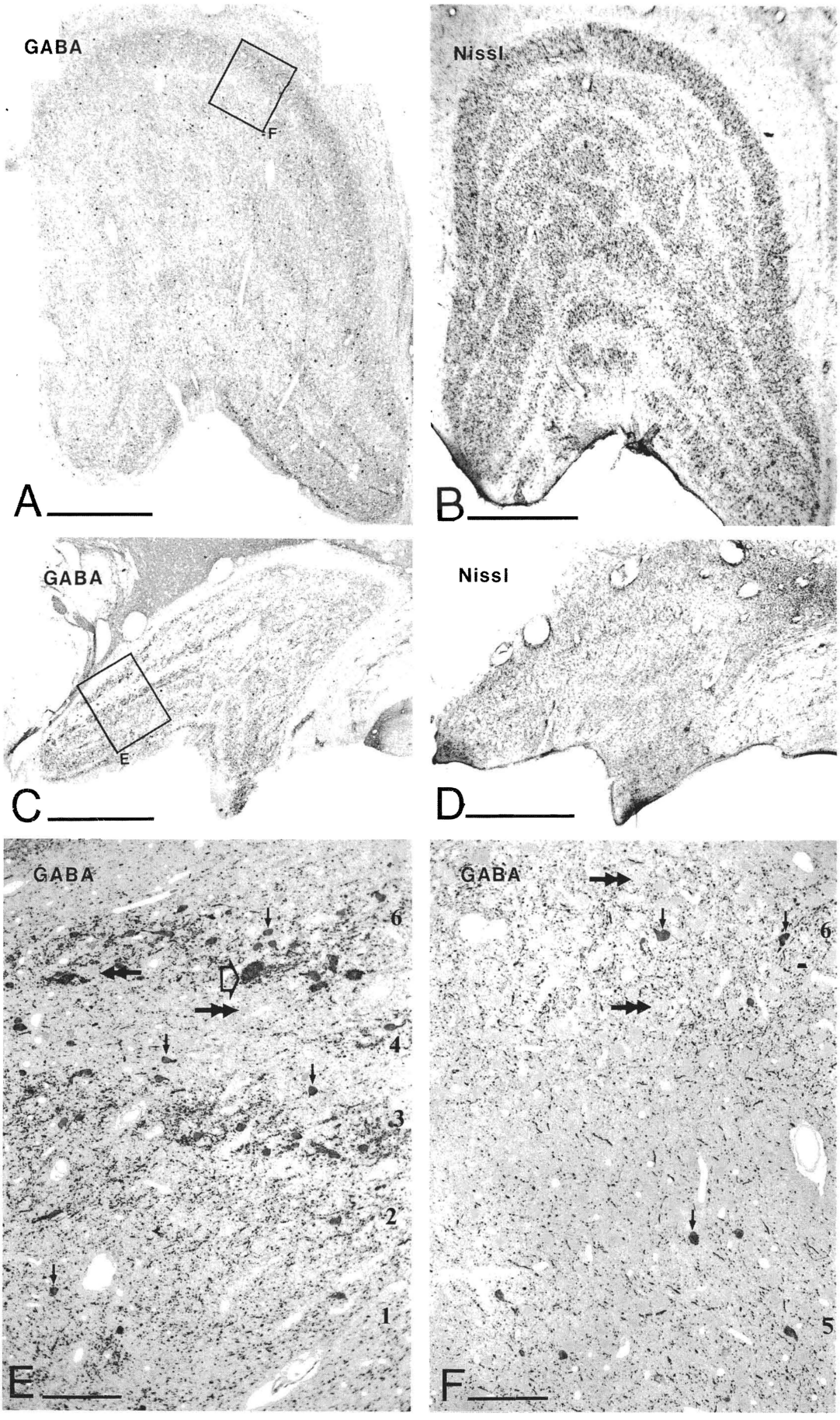

Fig. 3

magno- and parvo-cellular laminae (see Fig. 2). In size and morphology they were indistinguishable from cells known to be interneurons and shown previously to contain glutamate decarboxylase (GAD) (Hendrickson et al. 1983) or GABA (Montero 1986) They constituted the overwhelming majority of surviving cells and were never retrogradely labelled with HRP from cortex. Neurons of the other type had larger somata of about 10–25 μm in diameter and were often labelled with HRP transported retrogradely from the cortex. Although it was not our purpose to determine the proportion of these cells labelled from the cortex, it was clear that about half of them were conspicuously labelled in the caudal half of the nucleus. This does not imply that the unlabelled cells do not project to the region of the prelunate gyrus for our HRP implants were several mm apart and effective uptake may be restricted to the immediate vicinity of the implants. Furthermore, under oil immersion at a magnification of ×1000 sparse HRP reaction end-product could often be seen in cells that appeared to be unlabelled at low magnifications.

GABA-immunopositive neurons. Immunostaining for GABA of semithin (0.5 μm thick) sections taken at corresponding coronal levels showed that the small surviving cells are immunopositive for GABA and are probably inhibitory interneurons (Fig. 3C, E). In both left and right geniculates, GABA-immunopositive somata and neuropil elements that were presumably dendrites and axonal processes, were concentrated in the main laminae; a much lower density of GABA-immunoreactive structures was present in the interlaminar zones (Figs. 2, 3). In three closely neighbouring sections through the central portion of the geniculate on each side GABA-immunopositive somata were drawn under oil immersion at a magnification of ×1000 and their area measured. Every alternate grid of 100×100 μm was examined throughout the nucleus. On the normal side the mean area of 329 parvocellular and 135 magnocellular neurons was 131.2 μm^2 and 126.5 μm^2 respectively. On the degenerated side 356 parvocellular and 147 magnocellular GABA immunopositive somata were 77 μm^2 and 89.3 μm^2 respectively. These differences in size between the two sides were significant (parvo: $T = -28.3$, df 595, $p < 0.001$; magno: $T = -11.31$, df 199, $p < 0.001$. We also counted the total number of GABA immunopositive somata in one section through the centre of the dLGN. There were 375 and 302 somata in the normal and degenerated sides respectively. This reduction in numbers on the degenerated side seen in a single section must be much greater when the overall linear shrinkage of 40% is taken into account. GABA immunopositive interneurons have therefore decreased both in size and number.

GABA-immunonegative neurons. A separate population of cells that survived cortical ablation had larger somata, and about half of them were heavily labelled with HRP from cortex. Occasionally, the dendrites emerged from two poles of the soma to run parallel with the laminar borders while other labelled cells had dendrites that radiated in many directions from the parent soma. These neurons, whether labelled or unlabelled with HRP, never showed GABA-immunoreactivity, indicating that they were chemically different from the GABA-immunopositive small cells. Presumably all these neurons were projection neurons.

Electron microscopy of HRP-labelled, geniculo-cortical cells in the degenerated dLGN

Six out of several hundred HRP-labelled cells were examined from magno- and parvo-cellular regions. They were selected in order to include both parvocellular and magnocellular zones and because they were densely labelled and surrounded by abundant anterograde labelling from the retina. Three cells (Nos 3, 4 & 5 in Fig. 4) were definitely in either parvo-cellular lamina 4 or the interlaminar zone above it, and one cell was in the interlaminar region between the two magno-cellular layers (No 6 in Fig. 4). Although cell 3 is shown as being just within lamina 4 it should be noted that the laminar borders were determined from adjacent sections and that the border is not as sharp as in a normal dLGN. The exact laminar position of two cells (Nos 1 and 2 in Fig. 4) could not be determined unequivocally because of the lack of clear landmarks such as termination pattern of retinal afferents and densely packed projection neurons. However, their dorsal position within the caudal region of the dLGN suggests that these cells were within the parvocellular region of the dLGN, corresponding to the central few degrees of the retina. All six cells displayed similar features: a round pale nucleus, large numbers of small mitochondria, and abundant rough endoplasmic reticulum (Fig. 5). Like all other projection neurons in the dLGN of adult primates these cells were also rich in lipofuscin granules. The somata rarely received synapses and the few synaptic contacts were established by boutons with pleomorphic vesicles establishing type 2 synapses (F type boutons, Fig. 5B).

Synaptic input to dendrites of HRP-labelled cells. Our primary goal was to identify whether retinal terminals in a retrogradely degenerated dLGN establish synaptic contacts with surviving neurons that project to extrastriate visual cortex. Therefore, we thoroughly analyzed the input to the dendrites of these six retrogradely labelled cells in long series of sections. Retinal and other

Fig. 3. Adjacent GABA-immunoreacted (**A, C**) and Nissl stained (**B, D**) sections through the right (**A, B**) and the left, degenerated (**C, D**) dLGN. Both methods reveal lamination. Framed areas from **A** and **C** are shown at higher magnification in **E** and **F**. In the degenerated dLGN (**E**) note the increased density of GABA-immunopositive neurons (e.g. arrows), the almost total absence of GABA-immunonegative neurons (double arrows mark the only two neurons in this field) and the presence of GABA-immunopositive neuropil islands (e.g. open arrow) as opposed to the normal dLGN in **F**, which contains a high density of GABA-immunonegative cells (e.g. double arrows). Numbers indicate layering; layer 5 is absent at this level or has fused with layer 6. Scales: **A–D**, 1 mm; **E, F**, 100 μm

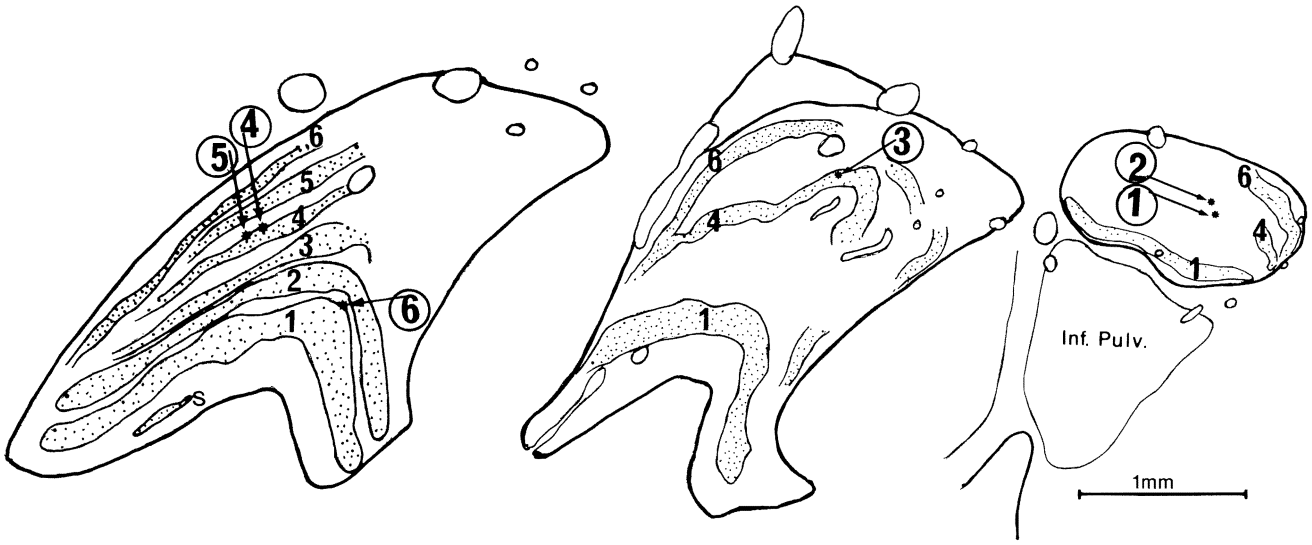

Fig. 4. Outline diagrams of sections through the left dLGN to show the positions of the 6 neurons (arrowed and circled large numbers) examined by electron microscopy. Laminae are indicated by smaller numbers. Cells 1 and 2 are close to the caudal pole, cell 3 is 600 μm rostral, and cells 4–6 are a further 500 μm rostral. The position of the laminae was determined from the TMB/HRP label and from autoradiographs for all 6 cells, from adjacent GABA-immunoreacted sections for cells 4–6, and from Nissl stained sections for cells 3–6

terminals were identified on the basis of well known fine structural criteria (Guillery and Collonier 1970; Hámori et al. 1974; Pasik et al. 1973); in addition some of the retinal terminals were also identified on the basis of HRP anterogradely transported from the eye. We are aware that such HRP labelling could arise by orthograde transport from the eye or the cortex, or by retrograde transport from cortex and thence by orthograde transport in a recurrent collateral of the labelled projection neuron. However, in monkeys both cortico-geniculate terminals (Guillery and Colonnier 1970; Pasik et al. 1973) and the terminals of projection neurons to striate cortex (Freund et al. 1987) contain small mitochondria with electron dense matrix. Therefore it is unlikely that any of the HRP-labelled terminals with pale mitochondria have a source other than the eye.

The dendrites often emitted thin appendages, some of which could be traced up to 10–15 μm from their origin. Both the main dendritic shafts and the appendages were densely covered by synaptic terminals. However none of about 250 synaptic boutons establishing contact with the retrogradely labelled geniculo-cortical neurons had the characteristic features of retinal terminals and only two were labelled by HRP. The paucity of any HRP labelling in these boutons may seem surprising in view of the extensive corticofugal projection to the dLGN. However, this corticofugal projection arises predominantly from striate cortex and was therefore destroyed by the lesion. The lack of retinal input was not due to the absence of retinal terminals in the area of the geniculo-cortical cells because the neuropile nearby contained both HRP-labelled and unlabelled synaptic terminals exhibiting the fine structural characteristics of retinal ganglion cell boutons. The dendrites of geniculo-cortical cells were densely surrounded by terminals of four different types, forming "synaptic islands" in the strongly gliotic tissue (Fig. 6).

1. The first type of element presynaptic to dendrites of geniculo-cortical cells could also be found postsynaptic to all other types of boutons, and probably corresponds to the presynaptic dendrites (F_2 bouton) of local circuit neurons. These presynaptic dendrites contained clear pleomorphic vesicles usually at a low density, and occasionally also larger vesicles with a granulated core. They formed type 2 synapses, but the extent of the postsynaptic density was variable (Fig. 6D). Presynaptic dendrites were rich in mitochondria and represented the most common presynaptic elements. Postembedding immunocytochemistry revealed that they were invariably immunopositive for GABA (Fig. 6C–E).

2. The second type of presynaptic element was always presynaptic only. These boutons contained vesicles similar to the first type of bouton, but generally at a higher density. Most of these terminals are probably axonal boutons of diverse origin and have been described as F_1 type boutons (Guillery and Colonnier 1970). Although common, they were less frequently encountered than the first type. They usually established type 2 synaptic contacts, but the thickness of the postsynaptic density was variable. These boutons often did not contain mitochondria in the plane of the section; in other cases the mitochondria were densely packed at the periphery of the bouton away from the synaptic contact. Many, but not all of these boutons were immunopositive for GABA, and usually they had the highest density of immunogold, demonstrating the highest levels of immunoreactive GABA. When the presynaptic profiles were small, F_1 and F_2 boutons could not always be distinguished even in GABA-immunoreacted sections (Fig. 6).

3. The third type of terminal was always presynaptic and relatively small, containing clear, round, densely packed vesicles (RSD type bouton, Guillery and Colonnier 1970; Szentágothai 1973). They established exclusively type 1 synapses, with both F_2 boutons (Fig. 6A)

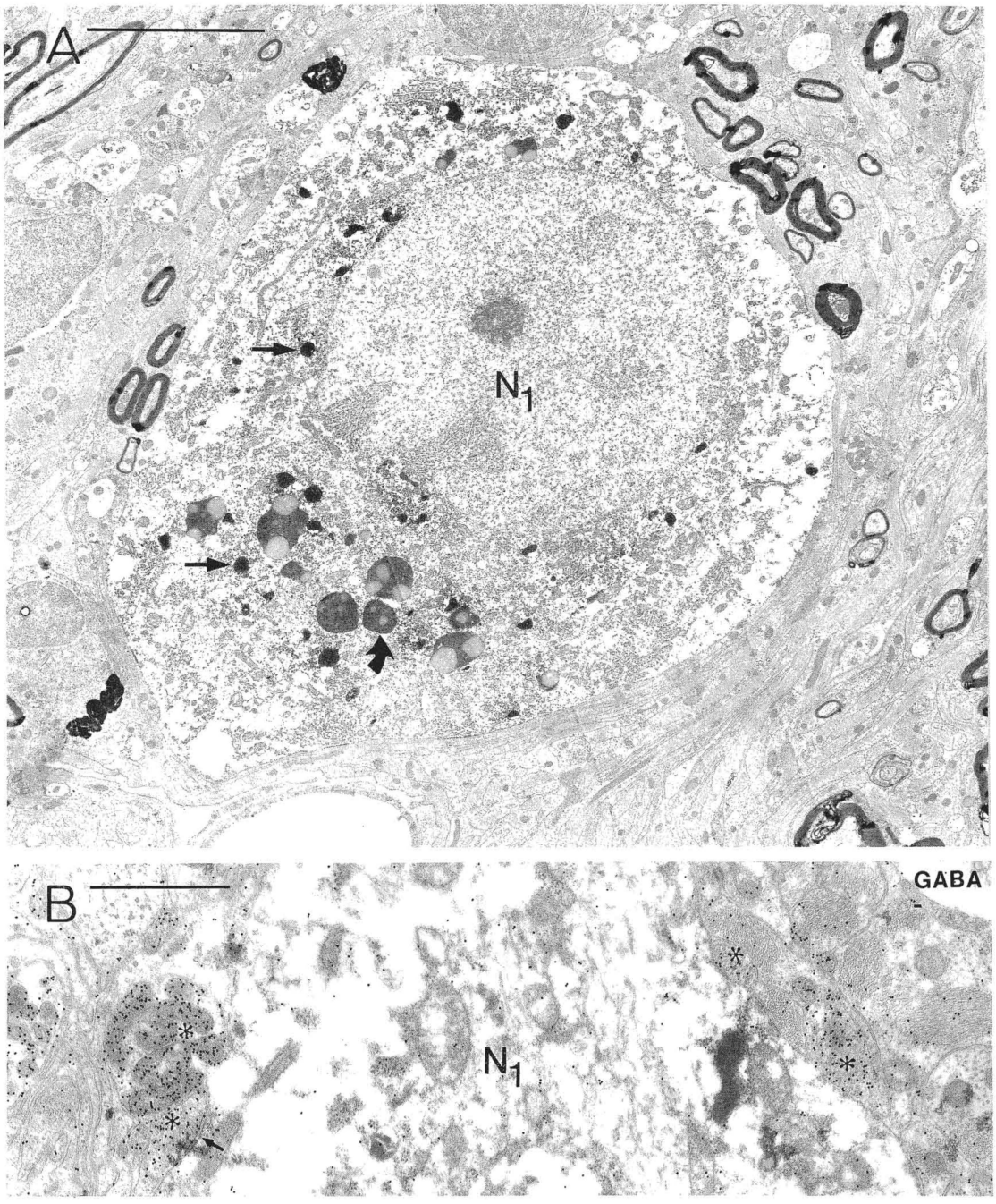

Fig. 5. A Electron micrograph of a geniculo-cortical cell (N_1) retrogradely labelled with HRP from the extra-striate visual cortex in the degenerated dLGN. The cell contains both granular (e.g. straight arrows) and diffuse HRP reaction endproduct and lipofuscin vacuoles (curved arrow). The cell body is encapsulated by glial processes which also dominate the neuropile. **B** Another section of the same cell illustrating that the scarce input to the soma is provided mainly by GABAergic terminals (asterisks). Several neuronal F type profiles, one of them making a type 2 synapse (arrow) with the geniculo-cortical cell, contain high density of colloidal gold particles following immunoreaction for GABA. Scales: **A** 5 μm; **B** 1 μm

and with dendrites of geniculo-cortical cells. As shown earlier (Pasik et al. 1973) many of them probably belong to corticofugal afferents originating from visual cortex. This is supported by the finding of two HRP-labelled terminals (not shown) one of which made a synapse with a large dendrite unlabelled by HRP or GABA. The synaptic junction of the other bouton was not identified. These terminals were never immunopositive for GABA.

In the normal dLGN RSD terminals constitute the majority of presynaptic elements. However, in the degenerated dLGN they were far outnumbered by other types of bouton, and this is compatible with the finding that only two HRP-labelled RSD terminals were found.

4. Terminals of the fourth type were always presynaptic and the boutons and their vesicles were larger than those of the third type. They often contained large vesi-

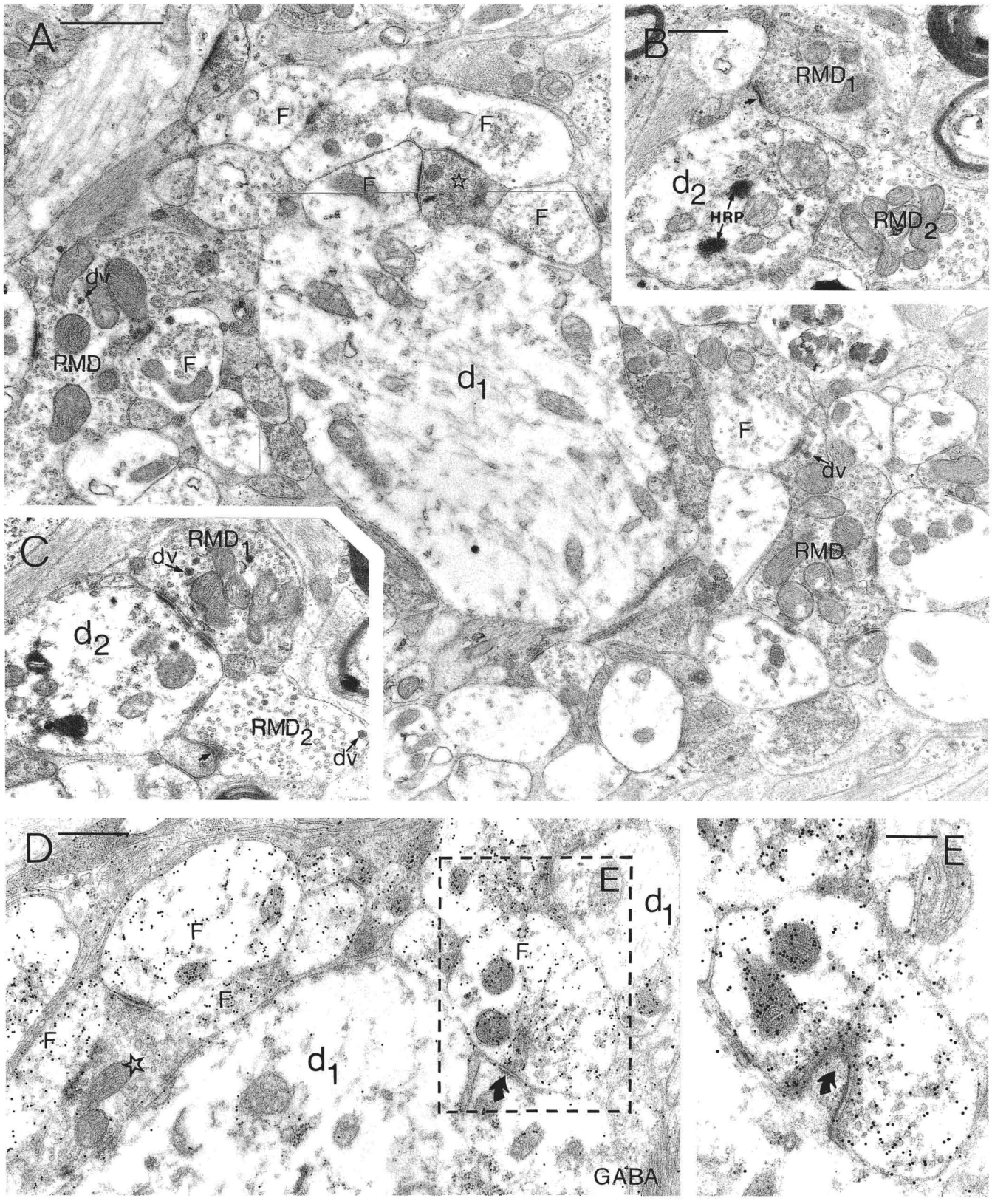

Fig. 6A–E. Synaptic input to the geniculo-cortical cell N1, also shown in fig. 5, in the parvo-cellular region of the degenerated dLGN. **A** A large dendritic trunk (d_1) in a synaptic "island" is surrounded by terminals, two of which receive synapses from an RSD type terminal (star). Note that many F terminals are post-synaptic to other boutons and correspond to presynaptic dendrites of local interneurons. Large RMD type terminals make synapses with many F profiles nearby. **B, C** Two RMD type terminals (RMD_1 and RMD_2) in serial sections establishing type I synapses on the shaft and on two spine-like protrusions (arrows) of an HRP-labelled proximal dendrite (d_2) of the same cell. Note that RMD terminals often contain dense core vesicles (dv), also seen in **A**. **D** GABA-immunoreacted serial section of dendrite, d_1 shown in **A**. With the exception of the RSD terminal (star), shown also in **A**, and dendrite d_1, all neuronal elements (e.g. F) show strong immunolabelling for GABA. Framed area is also shown in E in a serial section. **E** One of the GABA-immunopositive terminals is in synaptic contact (curved arrow) with the dendritic shaft and with a spine-like protrusion of the same dendrite. Scales: **A** 1 μm; **B, C,** 0.5 μm; **D**, 0.5 μm; **E**, 0.25 μm

cles with a granulated core and were never immunopositive for GABA. They most probably correspond to RMD (round vesicles, medium size dark mitochondria) terminals, named by Wilson and Hendrickson (1981) in the macaque dLGN. Although the latter authors found RMD terminals only in interlaminar zones 1–2 and 2–3, in our sample they occurred in the most dorsal parvocellular region as well. RMD terminals established multiple, type 1 contacts with F_2 and HRP-labelled dendrites, often in triadic arrangement similar to that formed by retinal axons in the normal dLGN. Although we made no quantitative measurements, it was estimated that F_1 and F_2 synaptic terminals constitute more than 50% of all synaptic contacts. Serial sections of the geniculo-cortical cell No 1 immunostained for GABA revealed that one of its dendritic segments received 12 RMD, 1 RSD, 14 F_2 and 4 F_1 synapses.

Other neuropil elements. Many of the myelinated axons in the degenerated, as well as in the normal, dLGN were GABA-immunopositive (Fig. 8B). It is therefore conceivable that some of the GABA-immunopositive terminals are of external origin. It was not, however, possible to determine whether they belong to axons of retinal afferents containing high levels of GABA or axons from GABAergic cells in the thalamic reticular nucleus. Additionally, local GABA cells may also contribute to these GABA-immunopositive myelinated axons.

A few axon terminals in both geniculate nuclei showed characteristics different from either of the above categories. These terminals were electron dense, contained small round vesicles and dark mitochondria. Some of them were strongly labelled for GABA, others were immunonegative.

Synaptic targets of identified retinal terminals (RLP)

Degenerated dLGN. The absence of retinal terminals making synapses with retrogradely HRP-labelled geniculo-cortical neurons lead us to analyze the postsynaptic targets of retinal terminals quantitatively (Table 1). Areas containing HRP-labelled neurons in magno- and parvo-cellular regions, including neighbouring interlaminar zones, were screened for anterogradely HRP-labelled or unlabelled retinal terminals in single sections many of which had been immunostained for GABA. The fact that not all retinal terminals are labelled is no surprise.

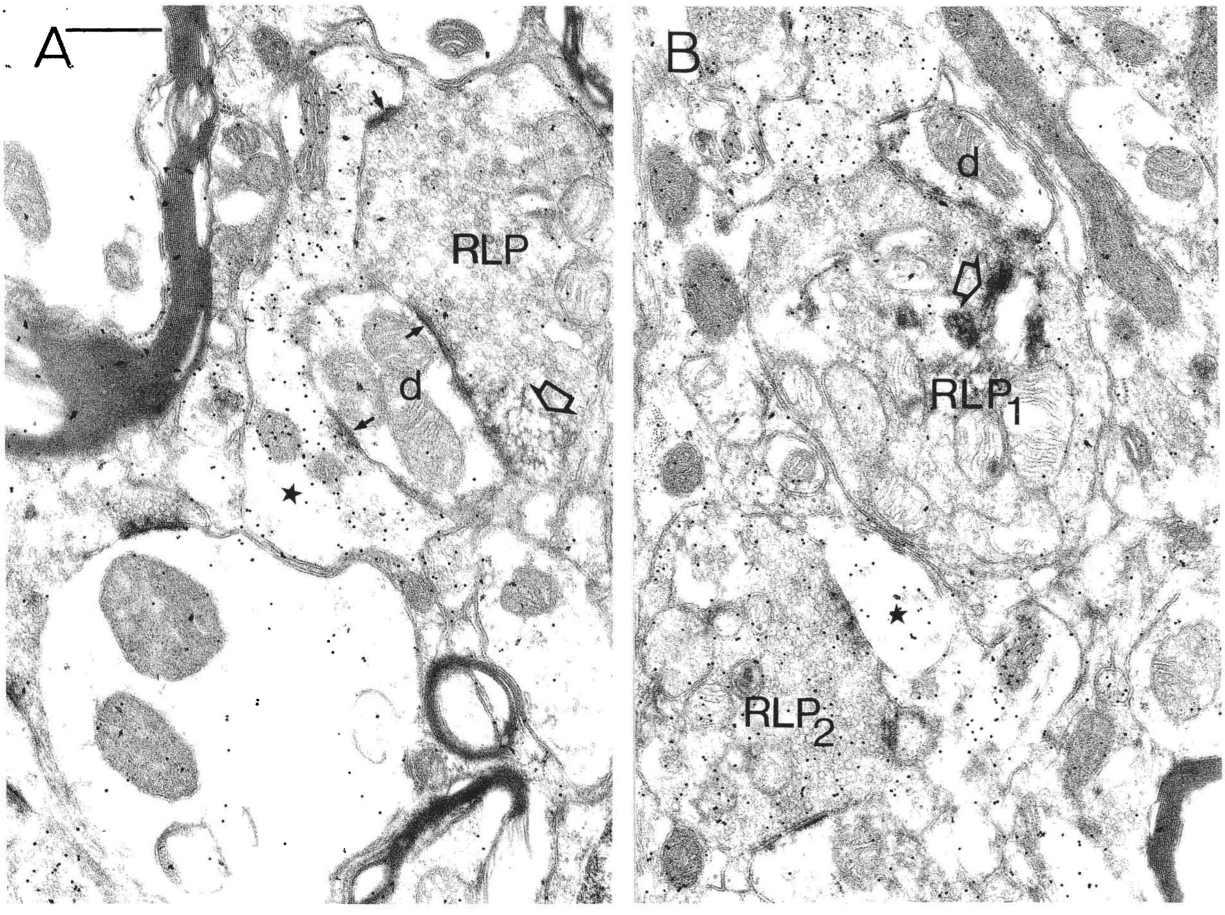

Fig. 7A, B. Postsynaptic targets of anterogradely HRP-labelled (open arrows) retinal terminals (RLP) in the normal dLGN. Each section was reacted for the presence of HRP and subsequently immunostained for GABA with the colloidal gold method. In the normal dLGN retinal terminals make synapses with GABA-immunonegative (d), and GABA-immunopositive (stars) dendrites, often forming "triadic" arrangement (arrows in **A**). One of the retinal terminals (RLP_2) has an immunogold density comparable to that of the F terminals and is considered GABA-immunopositive. Scale: **A, B,** 0.5 μm

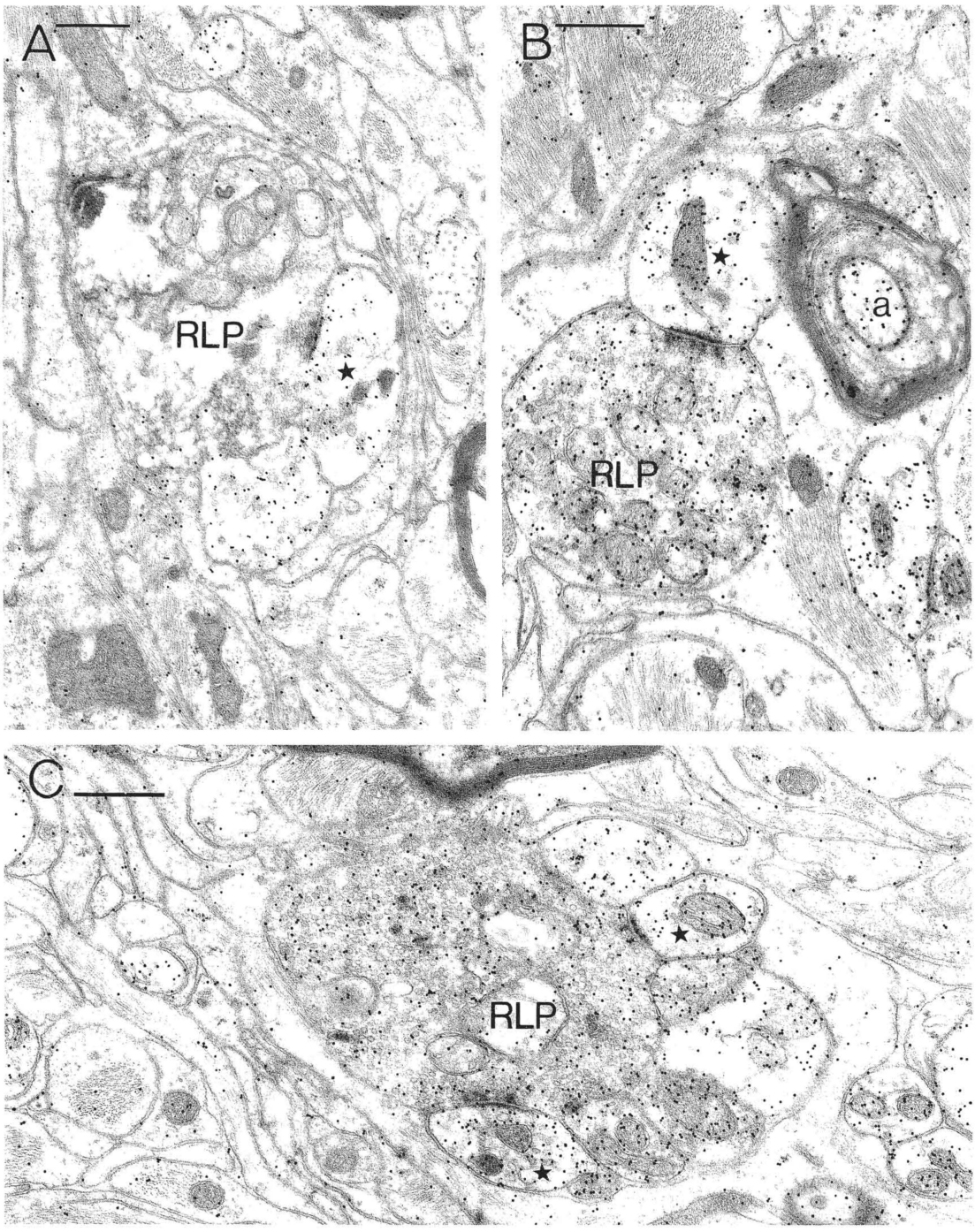

Fig. 8A–C. In the degenerated dLGN HRP-labelled (**A**) and unlabelled (**B, C**) retinal terminals (RLP) establish synapses exclusively with GABA-immunopositive vesicle containing dendrites (stars). Two of the RLP terminals in **B, C,** a myelinated axon (a) in **B** and many small profiles are immunopositive for GABA demonstrated by the high density of overlying immunogold particles. Scales: **A–C** 0.5 μm

HRP is not uniformly distributed throughout terminal branches and boutons and many sections are bound to miss it. Retinal terminals, whether HRP-labelled or unlabelled, were identified using ultrastructural criteria of large size, round vesicles, pale mitochondria (RLP type) and being always presynaptic, establishing type 1 contacts with their targets (Figs. 7, 8, 9). A total of 138 retinal terminals were encountered, making 201 synaptic contacts. On average, RLP terminals established synaptic contacts with 1.46 postsynaptic elements, as found on analysis of single sections.

A striking and unexpected finding was that all of the 167 postsynaptic targets tested were GABA-immunopositive vesicle-containing dendrites (Fig. 10). The remaining 34 postsynaptic elements, not reacted for GABA, were also vesicle-containing dendrites of the F_2

Table 1. Postsynaptic targets of HRP-labelled and unlabelled retinal terminals examined in electron microscopic sections. Most sections were immunoreacted for GABA. (* Vesicle-containing postsynaptic dendrite)

Layer	HRP-labelled retinal terminals						Unlabelled retinal terminals					
	GABA-reacted		GABA-positive		not reacted		GABA-reacted		GABA-positive		not reacted	
	Retinal terminal	Target	Retinal terminal	Target	Retinal terminal	Target	Retinal terminal	Target	Retinal terminal	Target	Retinal terminal	Target
DEGENERATED dLGN (left)												
Magno	56	83	7	83	16	25	11	12	4	12	5	9*
Parvo	36	51	11	51	0	0	14	21	4	21	0	0
Total	92	134	18	134	16	25	25	33	8	33	5	9*
NORMAL dLGN (right)												
Magno	33	50	0	7	4	6 (1*)	19	42	1	13	3	5
Parvo	28	45	0	4	0	0	0	0	0	0	0	0
Total	61	95	0	11	4	6 (1*)	19	42	1	13	3	5

type (Table 1). Interestingly, the only GABA-immunonegative presynaptic element in contact with these GABA-immunopositive and F_2 type dendrites was the retinal terminal (e.g. Fig. 8). Less frequently other F terminals also made synapses with these F_2 type dendrites.

Normal dLGN. Similar quantitative analysis was carried out on sections from the normal side (Table 1 and Fig. 10). The synaptic architecture was similar to that described in previous studies (Guillery and Colonnier 1970; Hámori et al. 1974; Pasik et al. 1973; Wilson, 1989; Wilson and Hendrickson 1981). On average, RLP terminals established synaptic contacts with 1.70 postsynaptic elements, as found on analysis of a total of 87 RLP terminals from single sections. Only 17.5% of the tested 137 postsynaptic elements were GABA-immunopositive dendrites for the 80 retinal terminals examined in magno- and parvo-cellular divisions (Table 1). This is in contrast with the degenerated dLGN where 100% of the retino-recipient elements were GABA-immunopositive (Fig. 10).

GABA-immunopositive retinal terminals

Some HRP-labelled and unlabelled RLP terminals from both geniculates showed selective accumulation of gold particles, indicating the presence of immunoreactive GABA (Figs. 7B, 8B, C, 9A, C). On the basis of the fine structural features described earlier for the primate (RLP, Guillery and Colonnier 1970) and also confirmed in the present study, these terminals can only be classified as boutons of retinal axons and their features were indistinguishable from those of nearby HRP-labelled and unlabelled GABA-immunonegative RLP type terminals (Fig. 7B). In order to establish whether there were two populations of retinal terminals with respect to GABA-immunoreactivity, as suggested by initial visual inspection, the density of immunogold particles was measured over all 197 GABA-immunoreacted retinal terminals of both dLGNs. As the postembedding immunogold technique can yield disparate absolute densities of gold particles from experiment to experiment, depending on many technical factors, the density of immunogold over retinal terminals was expressed in relation to the density over their nearby postsynaptic F_2 boutons in the same section. In a few cases 2 or 3 serial sections were averaged for the same profiles and the ratios were very similar from one section to another. The postsynaptic values are taken to represent the GABA-immunoreactivity of known GABAergic elements. The GABA-immunoreactivity in retinal terminals may then be expressed as the ratio of presynaptic: postsynaptic grain densities.

The relative GABA-immunoreactivity of retinal terminals found in the left and right dLGNs is plotted in the form of frequency histograms in Fig. 11A, B. Note that the distribution of ratios in the left degenerated dLGN differs from that found in the normal right dLGN, in a way which suggests that there may be more than one population of retinal terminals in the left dLGN. This was tested as follows. As ratios are unsuitable for direct statistical evaluation because of their skewed distribution they were subjected to a conventional arcsine transformation. One outlying value (> 1.0) was removed from the data set of each dLGN before the transformation was performed. The resulting distribution, shown in Fig. 11C, D, is clearly bimodal, and was found to depart significantly from normal using a Kolmogorov-Smirnov goodness-of-fit test ($D = 0.243$, $n = 116$, $p < 0.01$). The cut-off point between the two modal distributions was determined objectively using a maximum entropy thresholding technique (Johannsen and Bille 1981). Following back-transformation this point was found to correspond to a ratio of GABA-immunoreactivity of 0.273. When the transformed data from the degenerated and normal dLGNs were sorted into low and high immunoreactivity groups according to this criterion, none of the resulting unimodal distributions differed significantly from a normal distribution, and there was no significant difference between the treated and untreated (control) dLGNs in the values of the low reactivity groups (one-way ANOVA: $F = 2.8$, $df = 1$, $p = 0.096$). On the basis of this analy-

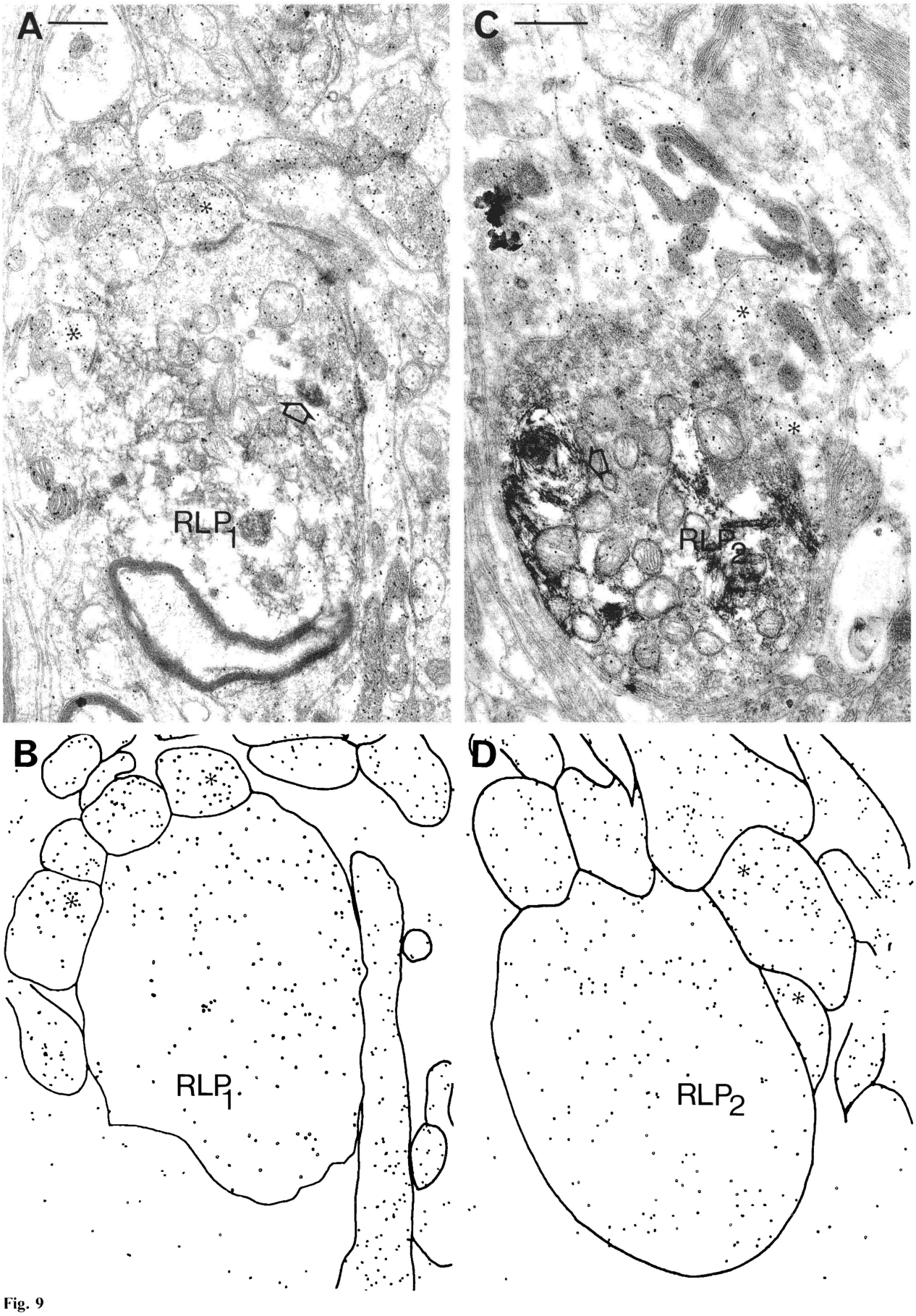

Fig. 9

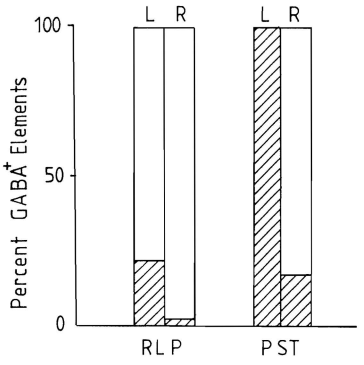

Fig. 10. The histogram shows the percentage of RLP terminals and their postsynaptic (PST) targets that were GABA-immunopositive (hatched areas) in the degenerated left and intact right dLGN. As only those sections that were reacted for GABA could be used, the data are a subset of those listed in Table 1

sis, we conclude that there were two classes of retinal terminals with respect to GABA-immunoreactivity in the degenerated dLGN. One class had a GABA-immunoreactivity which was not significantly different from that in the untreated, control dLGN. The other class consisted of terminals with a relatively high presynaptic GABA-immunoreactivity (i.e. values > 0.273, of which there were 26 (22%) in this sample), which were not represented in the untreated, control dLGN. These terminals may be thought of as belonging to a distinct high GABA-immunoreactivity group. Of the 117 retinal terminals from the degenerated dLGN, a total of 26,

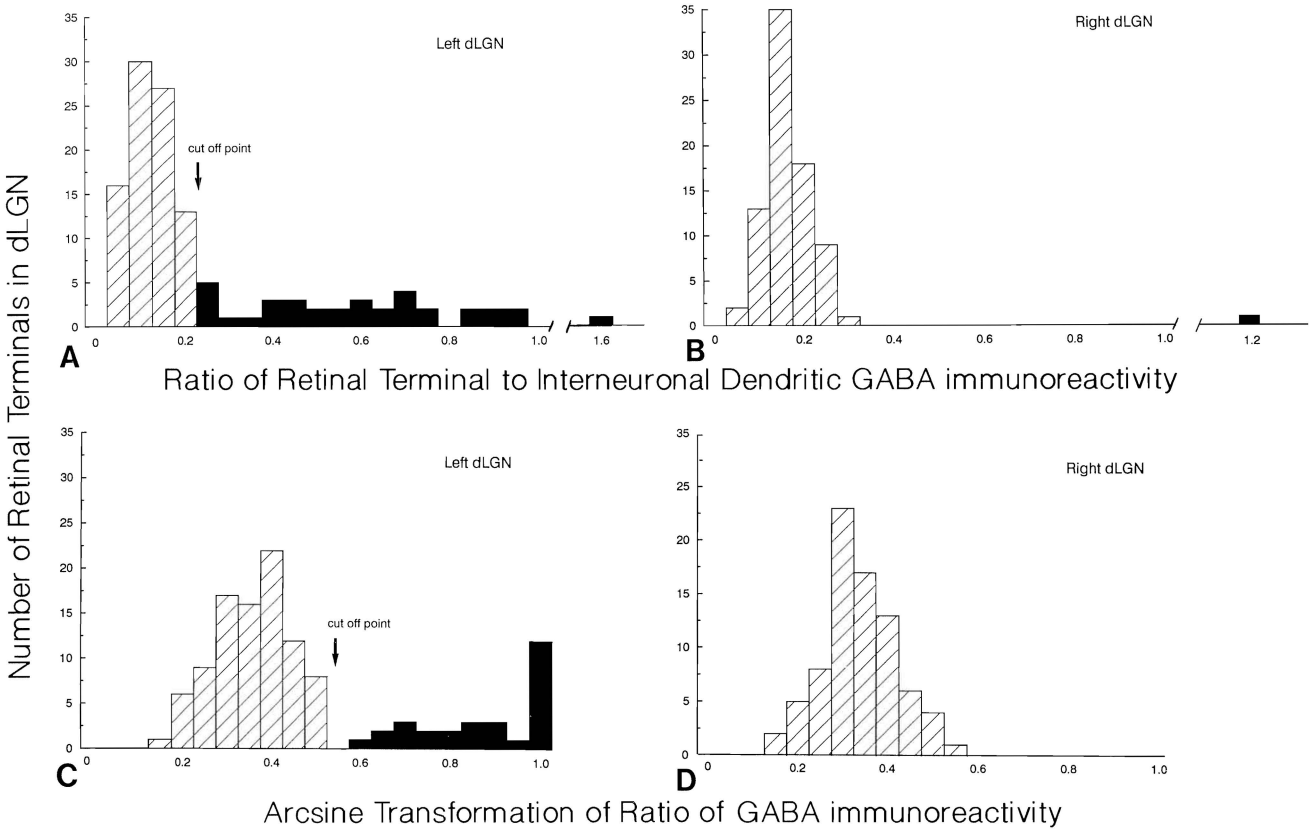

Fig. 11. A, B Show the ratio of the density of GABA-immunogold particles over retinal terminals and adjacent postsynaptic vesicle-containing F dendrites in degenerated (left) and normal (right) dLGN. Note the presence on the left of a population of retinal terminals (black) rich in GABA. **C, D** Show the arcsine transformation of the data from **A, B**. The arrow in **A, C** marks the objectively determined cut-off between two statistically different populations with respect to GABA-immunoreactivity

Fig. 9A–D. GABA-immunoreactivity of anterogradely HRP-labelled retinal terminals (RLP_1 and RLP_2) and their synaptic targets in the degenerated dLGN. Parvo- (**A, B**) and magno-cellular (**C, D**) regions of the degenerated dLGN were GABA-immunoreacted. The amorphous and crystalline deposit (open arrows), some of which was lost during processing for electron microscopy and thereby produced the cavities in the tissue, demonstrates HRP labelling from the eye. The accumulation of gold particles indicates GABA-immunopositive elements. The two retinal terminals establish synapses exclusively with GABA-immunopositive vesicle containing F_2 profiles (asterisks). The distribution of all gold particles is shown in **B, D,** to demonstrate that the retinal terminals have higher density than the surrounding neuropile. Note the similar density of immunolabelling over the retinal terminals and their immunopositive postsynaptic targets. Scales: **A–D,** 0.5 μm

(15% and 30% respectively of terminals in magno- and parvocellular regions) showed positive GABA-immunostaining as opposed to only 1 terminal (1.2%) in the normal side (Fig. 10). There was no indication that the reaction end-product of the transported HRP could produce false- positive GABA-labelling in RLP terminals. On the contrary, for some HRP-labelled RLP terminals the particle density was considerably lower over the TMB–AHM deposit (Fig. 9C), so that the proportion of GABA-immunopositive RLP terminals given in table 1 is probably an underestimate. Retinal terminals evidently contain lower levels of immunoreactive GABA than their postsynaptic dendrites originating from GABAergic neurons, because the density of gold over RLP


A
INL
IPL
G
P
Nissl
temporal
F
nasal
B
INL
IPL
G
P
GABA
F
C
G
IPL
INL
D
G
IPL
INL
G
P
GABA
F
E
GABA
F
GABA

Fig. 12

terminals was usually lower than that of F profiles. However, some RLP terminals, mainly of those unlabelled by HRP, had similar or even higher density of gold particles than their vesicle-containing GABA-immunoreactive targets (Fig. 8B)

Retinal histology

Horizontal sections through the fovea of the left eye, were stained with cresyl violet for Nissl substance (Fig. 12A). The most prominent feature is the retrograde transneuronal degeneration, involving about 80% of the ganglion cells in the central temporal hemiretina. The degeneration affected the entire hemiretina, as described before (Van Buren 1963; Cowey et al. 1989) although only the first 10 or so degrees are shown in Fig. 12. Sections reacted for GABA showed an unexpected strong immunoreactivity which was confirmed in all of several additional series of sections (Fig. 12B). In the intact nasal hemiretina GABA-immunostaining is clear in the inner plexiform layer and the inner nuclear (amacrine cell) layer, shown in more detail in Fig. 12D, where GABA-immunopositive cell bodies are seen both here and in the ganglion cell layers. The generally small size of the GABA-immunopositive neurons in the ganglion cell layer of the normal retina suggests that they are the well-known displaced amacrine cells, but the presence of GABA-immunopositive ganglion cells cannot be excluded. In the degenerated temporal hemiretina the GABA-immunoreactivity in the inner plexiform layer is much more intense and a population of larger GABA-immunopositive neurons is now prominent in the depleted ganglion cell layer (Fig. 12B, C). These naso-temporal differences are not present in several normal retinae we have examined (Fig. 12G). Finally, GABA-immunopositive axons were common in the optic nerve head of the experimental monkey (Fig. 11E) whereas they are rare in a normal eye of a macaque (Fig. 12F) processed in identical fashion. This observation is important because it suggests that GABA immunopositivity does occur in ganglion cells and that the numerous GABA-immunopositive terminals that were encountered in the degenerated dLGN represent an absolute increase rather than a relative increase resulting from the selective elimination of GABA-immunonegative terminals.

Fig. 12. Retina of the left eye from the monkey with striate cortex removal (**A–E**) is compared to the retina of a normal monkey (F–G). **A** Note the huge depletion of ganglion cells (**G**) in the temporal retina. **B** GABA-immunoreactivity of the inner plexiform layer (IPL) is increased from a point just nasal to the fovea to the far temporal retina. The dark line labelled P in figs. **B, G** is the pigment epithelium and it does not represent GABA-immunoreactivity. **C, D.** GABA-immunoreactivity is much stronger in the inner plexiform layer of the temporal retina (**C**) than in the apparently normal nasal retina (**D**). In both retinae small (arrows) and some large (double arrows) GABA-immunopositive neurons are present in the inner nuclear layer (INL) and in the ganglion cell layer (**G**). **E, F.** GABA-immunoreactive axons in the operated (**E**) and in a normal (arrows in **F**) optic nerve close to the vitreal surface. Note the increased density of GABA-immunopositive axons following striate cortex removal **G**. GABA-immunoreactivity in a normal retina does not show a naso-temporal difference. F = fovea. Scales: **A, B, G,** 1 mm; **C–F,** 5 μm

Discussion

Our results reveal a highly unusual pattern of retinal input to a degenerated dLGN, together with heightened levels of GABA in the transneuronally degenerated hemiretina. Are these remarkable features representative of the effects of long-term striate cortical damage in primates, or might we have fortuitously selected a rare animal? We have now examined retinal sections from a macaque monkey with a small bilateral ablation to the striate cortex representing the central five or so degrees of the retina and sections from three macaques in which parts of the optic tracts had been severed. The survival times were from just over one to several years. The elevated GABA levels were present in the degenerated parts of the retina of all four monkeys and GABA-immunopositive axons were present in the optic nerve head, as described here. These ancillary observations, together with the fact that the large surviving dLGN neurons projected to extrastriate cortex as reported earlier (Yukie and Iwai 1981) and received no direct retinal input as noted previously by Dineen et al. (1982) collectively indicate that our results are not unique to the monkey we chose to study.

GABAergic neurons are the targets of retinal terminals in the degenerated dLGN

The GABAergic neurons of the dLGN, which appear to be exclusively local circuit neurons (Montero 1986; Hendrickson et al. 1983; Szentágothai et al. 1966) are known to receive retinal input and many of their dendrites provide presynaptic inhibitory input to the dendrites of geniculo-cortical relay neurons in a triadic arrangement (Colonnier and Guillery 1964; Szentágothai 1973; Hámori et al. 1974; Wilson 1989). They can also have axons providing further GABAergic innervation (Pasik et al. 1973; Szentágothai et al. 1966), though in a recent intracellular study no such axons were found (Wilson 1989). As these neurons survive removal of striate cortex, with the loss of most projection neurons in the dLGN, the GABAergic cells become the major targets of surviving retinal terminals. It is surprising however that even when the retinal terminals are near to the dendrites of retrogradely labelled surviving geniculo-extra-striate cortical cells, or to other GABA-immunonegative dendrites, they do not appear to form synapses with them. Although we have not been able to trace the synaptic input to extreme distal dendrites of surviving projection cells in the degenerated dLGN it is unlikely that a substantial input from retinal terminals would be present since all retino-recipient dendrites were GABA-immunopositive, and therefore belonged to interneurons, whereas projection neurons were always GABA-immunonegative. Obviously further work is needed to establish the input to

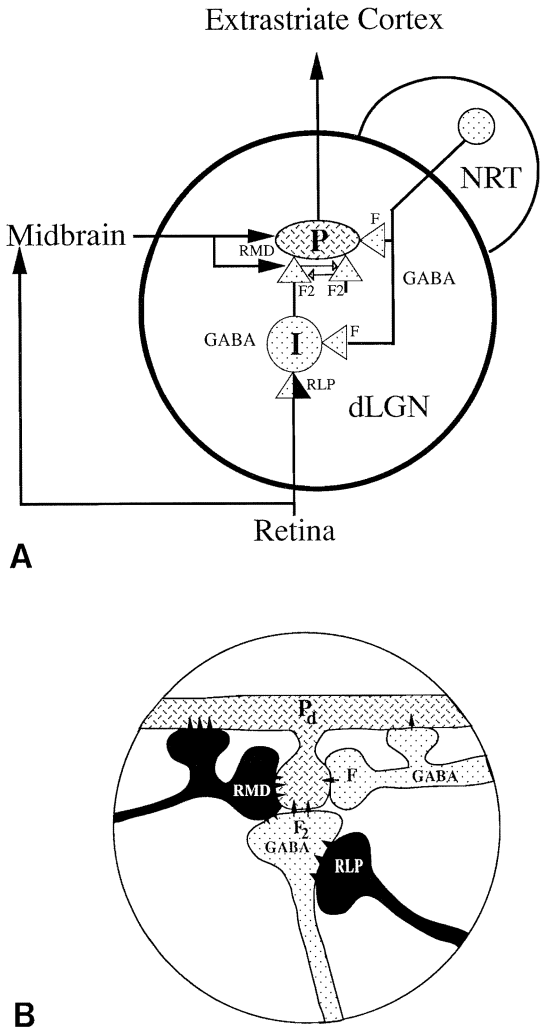

Fig. 13A, B. Schematic summary circuit diagram showing the connections of neurons (**A**) and their synaptic relationships (**B**) in the degenerated dLGN of the monkey. Dotted structures are GABA-immunopositive neurons. Note that in addition to the local interneurons (I) and a probably GABAergic input from the nucleus reticularis thalami (NRT, F terminals, Jones 1975; Hendrickson et al. 1983), a proportion of retinal terminals (RLP) are also GABA-immunopositive. Retinal terminals were not found in direct contact with projection neurons (P), instead the presumed mid-brain terminals (RMD) occupied their place in the triadic synaptic arrangements (**B**) that included the presynaptic dendrites (F_2) of the interneurons making synapses with dendrites (P_d) of projection neurons as well as with each other.

distal dendrites of identified interlaminar or type C cells both in the normal and in the degenerated dLGN. In this respect it is noteworthy that probably most of the surviving geniculate cells with extrastriate projections occupy the interlaminar zones, which receive very little retinal input (Benevento and Yoshida 1981; Wilson and Hendrickson 1981). Even the somata of C cells which lie in the main parvocellular laminae have dendrites that are nevertheless largely restricted to the interlaminar zones (Wilson and Hendrickson 1981). Therefore it is quite possible that in the normal as well as in the degenerated dLGN, these interlaminar cells receive no direct retinal input. Nonetheless, they are innervated by the GABAergic local circuit neurons which are activated monosynaptically by retinal input.

In the absence of cortical input, which was largely eliminated by striate cortical removal, the main non-GABAergic innervation of the geniculo-cortical cells seems to come from RMD terminals (Wilson and Hendrickson 1981), which presumably originate in the superior colliculus, although extrastriate cortical or thalamic origin cannot yet be excluded. Interestingly we found these terminals to be associated with GABA-immunopositive presynaptic dendrites in triadic arrangement to the projection neurons (see Fig. 13.), as has been shown for retinal terminals in the normal dLGN. Thus the interneurons supplying the presynaptic dendrites are activated by both retinal (non-triadic) and RMD terminals. We do not yet know whether the same interneurons receive both inputs, since convergence of retinal and RMD terminals has not been seen.

GABAergic retino-geniculate projection

In the normal dLGN of all species studied so far, stimulation of the retinal input to the dLGN leads to monosynaptic excitation of the target cells (Eysel 1976). It was therefore surprising to find that a significant population of retinal terminals in the degenerated dLGN contained immunoreactive GABA. The retinal origin of these terminals is evident from their HRP labelling and is also supported by the elevated density of GABA-immunopositive axons in the optic nerve of the experimental animal. Although the molecular identity of the immunoreactive substance cannot be unequivocally demonstrated by immunocytochemistry, it is unlikely that molecules other than GABA could be responsible for the reaction with the antibody for two reasons. First, glutamate, a transmitter amino acid present at high levels in retinal terminals (Montero and Wenthold 1989) and which is thought to mediate retino-geniculate transmission (Kemp and Sillito 1982; Crunelli et al. 1987) is not recognised by our antiserum (Hodgson et al. 1985). Second, the only molecule other than GABA that is known to be present in brain in significant amount and is recognised by our serum is beta-alanin. However, the serum reacts with beta-alanin at least ten times less effectively than with GABA. Therefore to achieve the same gold particle densities over genuinely GABA-storing elements and hypothetical beta-alanin-enriched retinal terminals the latter would have to contain a much higher concentration of beta-alanin than the concentration of GABA in GABAergic terminals. There is no evidence for selective stores of beta-alanin in the brain, but under abnormal circumstances such an unusual condition cannot be excluded.

It has been reported that in the rat up to 6% of ganglion cells that project to the superior colliculus were immunoreactive for GABA (Caruso et al. 1989), and in the rabbit a monoclonal antibody that recognises ganglion cells also reacted with GABA-immunopositive cells in the ganglion cell layer (Yu et al. 1988). In the primate however all GABA-immunopositive cells in the ganglion

cell layer have been thought to be displaced amacrine cells (Hendrickson et al. 1985; Wässle et al. 1989). Furthermore a previous immunocytochemical study showed that retinal terminals were rich in glutamate, but no GABA-immunopositive terminal was found in the same study (Montero and Wenthold 1989). However, our finding of one GABA-immunopositive out of 80 retinal terminals in the apparently normal right dLGN, and a few GABA-immunopositive axons in the normal optic nerve head, described previously (Koontz et al. 1989) and also found in our study, indicate that even the normal dLGN may receive a small GABAergic input from the retina in primates.

In contrast, in the degenerated retina, optic nerve and dLGN this GABAergic component is much more conspicuous. There are several possible explanations for this increase. For example, the GABAergic retino-thalamic projection may represent an expansion of the sparse normal projection due to hypertrophy of the axonal arbors in the dLGN. It is possible that the normal retino-geniculate axons expand, or that with the degeneration of most of the retinal terminals in the dLGN, retinal axons that normally innervate other brain areas colonise the atrophied dLGN. Alternatively, some ganglion cells which normally do not synthesize GABA in detectable amounts may change their neurotransmitter characteristics, upregulate GABA levels and survive preferentially in the retina. The possibility that the GABA we detected in retinal terminals derived from postsynaptic elements rather than being synthesised in the terminals is remote since there is no evidence to suggest that any terminal that is not GABAergic has the machinery for GABA uptake. Only further quantitative studies can show how this GABAergic projection is established.

The presence of GABA in retinal terminals prompts the question of how it is synthesised and whether it is released by visual stimulation and participates in synaptic transmission. Glutamate decarboxylase, the enzyme responsible for transmitter-GABA synthesis, has not been found in retinal terminals of the primate dLGN (Hendrickson et al. 1983), but if present in only a small minority of retinal terminals it could have been overlooked. Alternative biochemical pathways for GABA synthesis through gamma-hydroxybutyrate or putrescine are also known (for discussion see Sandler and Smith 1991), but whether retinal ganglion cells and their terminals can use these mechanisms remains to be established. GABA may not be the only neuroactive substance in these terminals, since GABA has been shown to coexist with other classical transmitters in the same nerve terminals. Thus cholinergic amacrine cells contain both GABA and its synthesizing enzyme glutamate decarboxylase (Vaney and Young 1988; Brecha et al. 1988) and they also release both GABA and ACh (O'Malley and Marshland 1989). Immunoreactive GABA has also been found in some cholinergic cortical terminals (Beaulieu and Somogyi 1990). Perhaps the most comparable condition has been reported in the hippocampus where the mossy fibres which produce monosynaptic EPSPs and are thought to use glutamate as transmitter have also been shown to be immunoreactive for GABA (Storm-Mathisen and Ottersen 1986; Sandler and Smith 1991). In the latter case there is no physiological evidence yet that GABA in mossy fibre terminals would participate in synaptic transmission. Only further physiological experiments can decide whether GABA is a neurotransmitter in the normal and altered retino-geniculate pathway.

Nevertheless, at present the most likely role for GABA in the retinal terminals is that of an inhibitory transmitter, and possible consequences of its action should be briefly considered. Since all the targets of the GABA-immunopositive retinal terminals were themselves GABA-immunopositive, GABA released from retinal terminals presumably disinhibits the targets of these inhibitory interneurons, including the geniculo-cortical projection cells. Thus the indirect action of GABAergic retinal terminals would be facilitatory on the projection cells, which will have lost much of their cortico-thalamic excitatory input as a result of the cortical ablation. GABAergic retinal input to the degenerated dLGN could therefore cause surviving projection neurons to increase their discharge rate. However, as interneurons also make extensive, and presumably inhibitory, synaptic contact with each other (Fig. 13) the GABAergic input to the dLGN could lead to a reduction in the discharge of particular projection neurons. It is worth noting that the action of GABA, whether released from retinal, interneuronal or other terminals, depends critically on the density and distribution of postsynaptic $GABA_A$ and $GABA_B$ receptors (Bowery et al. 1987). The $GABA_A$ receptor, which is present at particularly high density on certain projection neurons in the dLGN of the cat (Soltész et al. 1990), has been shown to play a major role in neurotransmission there (for review see Crunelli et al 1988). Therefore, if the projection cells in the monkey are also more richly supplied with $GABA_A$ receptors than the interneurons, they may be exquisitely sensitive to the inhibitory and disinhibitory processes that take place in the degenerated dLGN. These considerations should not draw attention away from the fact that the majority of retinal terminals remain GABA-immunonegative and presumably excitatory, and that these too can either inhibit surviving projection neurons via an interneuron, or disinhibit them via a chain of two inhibitory interneurons.

Implications for residual vision

Our results point to a retino-colliculo-geniculate pathway to area V4 (and perhaps V2) which survives damage to striate cortex. The retinal projection to the colliculus has often been invoked in the mediation of residual visual functions. The experiments of Mohler and Wurtz (1977) who showed that monkeys with striate cortical damage could still direct their eyes to targets presented within their field defects, but lost this ability after subsequent damage to topographically corresponding parts of the colliculus, demonstrate the particular importance of this projection. It is known that the colliculus projects to the pulvinar complex of the thalamus, which also receives a direct retinal input, and that the information may, via the

extensive pulvino-cortical projections, reach extra-striate visual cortical areas. The latter, especially area MT, are presumably involved in some aspects of residual vision since the residual ability to discriminate direction of movement following occipital damage is not present when an entire cerebral hemisphere is removed (Ptito et al. 1991).

The collicular projection to the dLGN may provide an alternative route to extrastriate visual areas. Our results show that surviving dLGN neurons, retrogradely labelled from some of these areas, receive a direct synaptic input from RMD terminals that are characteristic of the collicular projection to the dLGN (Wilson and Hendrickson 1981). It is not yet known whether neurons in, for example, V4 retain their visual responsiveness after striate cortical lesions, particularly in awake monkeys and after allowing sufficient time for possible long term adaptive changes after the lesion. Area V4 is part of the occipito-temporal cortical visual system within which both areas V2 and IT have been reported to lose all visual responsiveness, V2 immediately after cooling of striate cortex (Girard and Bullier 1989; Schiller and Malpeli 1977a), and IT and V4, at least under anaesthesia, after striate cortex ablation or cooling (Roch-Miranda et al. 1975; Girard et al. 1991). If V4 retains its responsiveness, it may provide additional input to area MT (Ungerleider and Desimone 1986) where visually responsive neurons remain after striate cortical damage (Rodman et al. 1989), or to any other of its multiple projection areas.

The importance of the dLGN in residual vision has been demonstrated by experiments of Schiller et al. (1990) who showed that monkeys with dLGN lesions involving all layers could not saccade to near threshold stimuli presented within the field defects even though the collicular receptive fields were still present. This striking and apparently permanent deficit implies that the colliculo-pulvinar projection alone cannot mediate saccadic localization even in the presence of a striate cortex whose geniculate input has been removed, or that its normal role is inhibited by the geniculate lesion. In either case, and taken together with the findings of Mohler and Wurtz (1977) this points to the colliculo-geniculate projection whose retinal input comes predominently from Pγ cells and possibly from Pα cells (Leventhal et al. 1981; Perry and Cowey 1984). The ultrastructural features and the GABA-immunonegativity of the RMD terminals in the degenerated dLGN which are presumably of collicular origin, make it likely that this input is excitatory.

In addition, we have provided evidence for a retinal projection, via GABA-immunopositive interneurons, to surviving dLGN cells that project to area V4 and possibly to other extra-striate cortical areas. This projection is present in both parvo- and magnocellular subdivisions, suggesting that both colour-opponent and broadband channels may contribute to the projection. However, it was not possible to determine whether the surviving projection neurons that we examined were from laminar or interlaminar regions; possibly all were interlaminar. The physiological properties of interlaminar dLGN neurons are poorly understood even in the normal dLGN, but there is evidence that those of the intercalated layer between the parvo- and magnocellular regions project to the cytochrome oxidase blobs in area V1 (Fitzpatrick et al. 1983; Livingstone and Hubel 1982) which are presumed to be involved in the processing of wavelength information. Interestingly, their retinal input, like that of the other interlaminar layers, is physiologically W-like in Galago and therefore characteristic of Pγ cells (Irvin et al. 1986). The little that is known about the functional properties of Pγ retinal ganglion cells does not indicate that they are particularly involved in the processing of wavelength information (de Monasterio 1978a), and even the broad wavelength tuning reported for collicular units (Kadoya et al. 1971) could be of cortical rather than retinal origin. If these cells provide a major input to the blobs – which have been dubbed the colour system of the striate cortex despite the fact only 60–70% of their cells are tuned to wavelength – we have either underestimated their wavelength specificity, or they sharpen their broad-band characteristics, e.g. by opponent interactions prior to cortex much as the broad tuning of retinal receptors is sharpened at later stages. The first alternative is possible because functional subclasses of Pγ cells may exist that have not yet been described. The second possibility is also consistent with our finding that surviving projection neurons in the degenerated dLGN receive direct, and probably excitatory input, from the superior colliculus and indirect, inhibitory, input via interneurons that are themselves postsynaptic to retinal terminals. The input from GABA-immunopositive interneurons may narrow the response tuning to the excitatory collicular input. This would be in accordance with generally accepted notions about the role of GABA which is thought to participate in centre-surround antagonism, providing spatial, directional, and chromatic tuning. The relative increase in GABA-immunopositivity in the degenerated dLGN, where 26 out of 117 retinal terminals examined were positive, compared with only 1 out of 80 in the normal dLGN, indicates that this tuning may also be present in Blindsight despite the massive cell loss caused by retrograde degeneration. Indeed, evidence for fairly sharp spatial (Stoerig and Cowey 1989a), orientational (Weiskrantz 1989), and chromatic tuning (Stoerig and Cowey 1989b, 1990) has been reported in blindsight.

Acknowledgements. The authors are grateful for the expert technical assistance of Mr. F. Kennedy, Mr. J.D.B. Roberts and Ms Eva Tóth. We also thank Dr. P. Azzopardi for statistical advice and assistance, Dr. Ulf T. Eysel for providing computing facilities for quantitative analysis and Ms. M. Bannister for her help in measuring the size of GABA-immunopositive neurons.. The research was supported by the Medical Research Council and by a European Science Foundation Visiting Fellowship to P. Stoerig and by a travel grant from the McDonnell-Pew Centre for Cognitive Neuroscience in Oxford.

References

Benevento LA, Standage GP (1982) Demonstration of lack of dorsal lateral geniculate nucleus input to extrastriate areas MT and Visual 2 in the macaque monkey. Brain Res 252:161–166

Benevento LA, Yoshida K (1981) The afferent and efferent organization of the lateral geniculo-prestriate pathways in the macaque monkey. J Comp Neurol 203:455–474

Bowery NG, Hudson AL, Price GW (1987) $GABA_A$ and $GABA_B$ receptor site distribution in the rat central nervous system. Neuroscience 20:365–383

Brecha N, Johnson D, Peichl L, Wässle H (1988) Cholinergic amacrine cells of the rabbit retina contain glutamate decarboxylase and γ-aminobutyrate immunoreactivity. Proc Nat Acad Sci USA 85:6187–6191

Bullier J, Kennedy H (1983) Projection of the lateral geniculate nucleus onto cortical area V2 in the macaque monkey. Exp Brain Res 53:168–172

Caruso DM, Owczarzak MT, Goebel DJ, Hazlett JC, Pourcho RG (1989) GABA-immunoreactivity in ganglion cell of the rat retina. Brain Res 476:129–134

Colonnier M, Guillery RW (1964) Synaptic organization in the lateral geniculate nucleus of the monkey. Z Zellforsch 62:333–355

Cowey A, Stoerig P (1989) Projection patterns of surviving neurons in the dorsal lateral geniculate nucleus following discrete lesions of striate cortex: implications for residual vision. Exp Brain Res 75:631–638

Cowey A, Stoerig P, Perry VH (1989) Transneuronal retrograde degeneration of retinal ganglion cells after damage to striate cortex in macaque monkeys: selective loss of Pβ cells. Neuroscience 29:65–80

Crunelli V, Kelly JS, Leresche N, Pirchio M (1987) On the excitatory post-synaptic potential evoked by stimulation of the optic tract in the rat lateral geniculate nucleus. J Physiol 384:603–618

Crunelli V, Haby M, Jassik-Gerschenfeld D, Leresche N, Pirchio M (1988) Cl^- and K^+ dependent inhibitory postsynaptic potentials evoked by interneurones of the rat lateral geniculate nucleus. J Physiol 399:153–176

de Monasterio FM (1978a) Center and surround mechanisms of opponent-color X and Y ganglion cells of retina of macaques. J Neurophysiol 41:1418–1434

de Monasterio FM (1978b) Properties of ganglion cells with atypical receptive-field organization in retina of macaques. J Neurophysiol 41:1435–1449

Dineen JT, Hendrickson AE (1981) Age-correlated differences in the amount of retinal degeneration after striate cortex lesions in monkeys. Invest Opthalmol Vis Sci 21:749–752

Dineen JT, Hendrickson A, Keating EG (1982) Alterations of retinal inputs following striate cortex removal in adult monkey. Exp Brain Res 47:446–456

Eysel UT (1976) Quantitative studies of intracellular potentials in the lateral geniculate nucleus of the cat with respect to optic tract stimulus response latencies. Exp Brain Res 25:469–486

Fitzpatrick D, Itoh K, Diamond IT (1983) The laminar organisation of the lateral geniculate body and the striate cortex in the squirrel monkey (Saimiri sciureus). J Neurosci 3:673–702

Freund TF, Martin KAC, Soltész I, Somogyi P, Whitteridge D (1987) Innervation of monkey striate cortex by physiologically identified and HRP-filled thalamocortical afferents. Soc Neurosci Abstr 13:1044

Fries W (1981) The projection from the lateral geniculate nucleus to the prestriate cortex of the macaque monkey. Proc Natl Acad Sci USA 213:73–80

Girard P, Bullier J (1989) Visual activity in V2 during reversible inactivation of area 17 in the macaque monkey. J Neurophysiol 62:1287–1302

Girard P, Salin PA, Bullier J (1991) Visual activity in macaque area V4 depends on area 17 input. Neuroreport 2:81–84

Guillery RW, Colonnier M (1970) Synaptic patterns in the dorsal lateral geniculate nucleus of the monkey. Z Zellforsch 103:90–108

Hámori J, Pasik T, Pasik P, Szentágothai J (1974) Triadic synaptic arrangements and their possible significance in the lateral geniculate nucleus of the monkey. Brain Res 80:379–393

Hendrickson AE, Dineen JT (1982) Hypertrophy of neurons in the dorsal lateral geniculate nucleus following striate cortex lesions in infant monkeys. Neurosci Letts 30:217–222

Hendrickson AE, Ogren MP, Vaughn JE, Barber RP, Wu J-Y (1983) Light- and electron microscopic immunocytochemical localization of glutamic acid decarboxylase in monkey geniculate complex. Evidence for GABAergic geniculate neurons and synapses. J Neurosci 3:1245–1262

Hendrickson A, Ryan M, Noble B, Wu J-Y (1985) Localization of gamma aminobutyric acid (GABA)-containing neurons in Macaca monkey and human retina. Invest Ophthalmol Vis Sci (Suppl) 26:95

Hodgson AJ, Penke B, Erdei A, Chubb IW, Somogyi P (1985) Antisera to γ-aminobutyric acid. I. Production and characterization using a new model system. J Histochem Cytochem 33:229–239

Huerta MF, Harting JK (1984) The mammalian superior colliculus: studies of its morphology and connections. In: Vanegas H (ed) Comparative neurology of the optic tectum. Plenum, New York, pp 687–773

Irvin GE, Norton TT, Sesma MA, Cassagrande VA (1986) W-like properties of interlaminar zone cells in the lateral geniculate nucleus of a primate (Galago crassicaudatus). Brain Res 362:254–270

Johannsen G, Bille J (1982) A threshold selection method using information measures. Proc 6th Int Conf Pattern Recognition 1:140–142

Kadoya S, Wolin LE, Massopust LC (1971) Collicular unit responses to monochromatic stimulation in squirrel monkey. Brain Res 32:251–254

Keating EG (1979) Rudimentary color vision in the monkey after removal of striate and preoccipital cortex. Brain Res 179:379–384

Kemp JA, Sillito AM (1982) The nature of the excitatory transmitter mediating X and Y cell inputs to the cat dorsal lateral geniculate nucleus. J Physiol 323:377–391

Kisvárday ZF, Cowey A, Stoerig P, Somogyi P (1990) Synaptic input of residual cells in the monkey lateral geniculate nucleus after striate cortex removal. Eur J Neurosci Suppl 3:245

Koontz MA, Hendrickson AE, Ryan MK (1989) GABA-immunoreactive synaptic plexus in the nerve fibre layer of primate retina. Vis Neurosci 2:19–25

Leventhal AG, Rodieck EW, Dreher B (1981) Retinal ganglion cell classes in oldworld monkeys: morphology and central connections. Science 213:1139–1142

Liposits ZS, Sétáló GY, Flerkó B (1984) Application of the silver-gold intensified 3,3′-diaminobenzidine chromogen to the light and electron microscopic detection of the luteinizing hormone-releasing hormone system of the rat brain. J Neurosci 13:513–525

Livingstone M, Hubel DH (1988) Segregation of form, colour, movement and depth: anatomy, physiology and perception. Science 240:740–750

Livingstone M, Hubel DH (1982) Thalamic imputs to cytochrome oxidase-rich regions in monkey visual cortex. Proc Natl Acad Sci USA 79:6098–6101

Merigan WH, Eskin TA (1986) Spatio-temporal vision of macaques with severe loss of Pβ retinal ganglion cells. Vision Res 26:1751–1761

Mihailovic LT, Dragoslava C, Dekleva N (1971) Changes in the number of neurons and glial cells in the lateral geniculate nucleus of the monkey during retrograde cell degeneration. J Comp Neurol 142:223–230

Mohler CW, Wurtz RH (1977) Role of striate cortex and superior colliculus in the guidance of saccadic eye movements in monkeys. J Neurophysiol 40:74–94

Montero VM (1986) The interneuronal nature of GABAergic neurons in the lateral geniculate nucleus of the rhesus monkey: a combined HRP and GABA-immunocytochemical study. Exp Brain Res 64:615–622

Montero VM, Wenthold RJ (1989) Quantitative immunogold analysis reveals high glutamate levels in retinal and cortical

synaptic terminals in the lateral geniculate nucleus of the macaque. Neuroscience 31:639–647
Olucha F, Martinez-Garcia F, Lopez-Garcia C (1985) A new stabilizing agent for the tetramethyl benzidine (TMB) reaction product in the histochemical detection of horseradish peroxidase (HRP). J Neurosci Meth 13:131–138
O'Malley DM, Masland RH (1989) Co-release of acetylcholine and -aminobutyric acid by a retinal neuron. Proc Natl Acad Sci 86:3414–3418
Pasik P, Pasik T, Hámori J, Szentágothai J (1973) Goldi type II interneurons in the neuronal circuit of the monkey lateral geniculate nucleus. Exp Brain Res 17:18–34
Perry VH, Cowey A (1984) Retinal ganglion cells that project to the superior colliculus and pretectum in the macaque monkey. Neuroscience 12:1125–1137
Perry VH, Linden R (1982) Evidence for dendritic competition in the developing retina. Nature 297:683–685
Perry VH, Oehler R, Cowey A (1984) Retinal ganglion cells that project to the dorsal lateral geniculate nucleus in the macaque monkey. Neuroscience 12:1101–1123
Ptito A, Lepore F, Ptito M, Lassonde M (1991) Target detection and movement discrimination in the blind field of hemispherectomized patients. Brain 114:497–512
Rocha-Miranda CE, Bender DB, Gross CG, Mishkin M (1975). Visual activation of neurons in inferotemporal cortex depends on striate cortex and forebrain commissures. J Neurophysiol 38:475–491
Rodman HR, Gross CG, Albright TD (1989) Afferent basis of visual response properties in area MT of the macaque. II. Effects of superior colliculus removal. J Neurosci 10:1154–1164
Sandler P, Smith AD (1991) Co-existence of GABA and glutamate in mossy fibre terminals of the primate hippocampus: an ultrastructural study. J Comp Neurol 303:177–192
Schilder P, Pasik P, Pasik T (1972) Extrageniculostriate vision in the monkey. III. Circle vs. triangle and "red vs. green" discrimination. Exp Brain Res 14:436–448
Schiller PH, Malpeli JG (1977a) The effects of striate cortex cooling on area 18 cells in the monkey. Brain Res 126:366–369
Schiller PH, Malpeli JG (1977b) Properties and tectal projections of monkey retinal ganglion cells. J Neurophysiol 40:428–445
Schiller PH, Logothetis N, Charles ER (1990) Role of the color-opponent and broad-band channels in vision. Vis Neurosci 5:321–346
Shapley R, Perry VH (1986) Cat and monkey retinal ganglion cells and their functional roles. Trends Neurosci 9:229–235
Soltész I, Roberts JDB, Takagi H, Richards JG, Mohler H, Somogyi P (1990) Synaptic and non-synaptic localization of benzodiazepine/GABA–A receptor/CL-channel complex using monoclonal antibodies in the dorsal lateral geniculate nucleus of the cat. Eur J Neurosci 2:414–429
Somogyi P (1988) Immunocytochemical demonstration of GABA in physiologically characterized, HRP-filled neurons and in their postsynaptic targets. In: van Leeuwen FW, Buijs RM, Pool CW, Pach O (eds.) Molecular neuroanatomy. Techniques in the behavioural and neural sciences. Elsevier, Amsterdam pp 3:339–359
Sternberger LA, Hardy PH Jr, Cuculis JJ, Meyer HG (1970) The unlabelled antibody enzyme method of immunohistochemistry. Preparation and properties of soluble antigen-antibody complex (horseradish peroxidase–anti-horseradish peroxidase) and its use in identification of spirochaetes. J Histochem Cytochem 18: 315–333
Stoerig P, Cowey A (1989a) Residual target detection as a function of stimulus size. Brain 112:1123–1139
Stoerig P, Cowey (1989b) Wavelength sensitivity in blindsight. Nature 342:916–918
Stoerig P, Cowey A (1990) Wavelength discrimination in blindsight. Invest Ophthal Vis Sci 31:189
Stoerig P, Zrenner E (1989) A pattern-ERG study of transneuronal retrograde degeneration in the human retina after a post-geniculate lesion. In: Kulikowski JJ, Dickinson CM, Murray JJ (eds) Seeing contour and colour. Pergamon, Oxford pp 553–556
Storm-Mathisen J, Ottersen OP (1986) Antibodies against amino acid neurotransmitters. In: Panula P, Paivarinta H, Soinila S (eds.) Neurohistochemistry: modern methods and applications, Alan R. Liss Inc. New York pp 107–136
Szentágothai J (1973) Neuronal and synaptic architecture of the lateral geniculate body. In: Jung R (ed) Handbook of sensory physiology, Springer Heidelberg, pp 141–176
Szentágothai J, Hámori J, Tömböl T (1966) Degeneration and electron microscope analysis of the synaptic glomeruli in the lateral geniculate body. Exp Brain Res 2:283–301
Ungerleider LG, Desimone R (1986) Cortical connections of visual area MT in the macaque. J Comp Neurol 248:190–222
Van Buren JM (1963) Trans-synaptic retrograde degeneration in the visual system of primates. J Neurol Neurosurg Psychiat 26:402–409
Vaney DI, Young HM (1988) GABA-like immunoreactivity in cholinergic amacrine cells of the rabbit retina. Brain Res 438:369–373
Wässle H, Grunert U, Rohrenbeck J, Boycott BB (1989) Cortical magnification factor and the ganglion cell density of the primate retina. Nature 341:643–646
Weber JT, Huerta MF, Kaas JH, Harting JK (1983) The projections of the lateral geniculate nucleus of the squirrel monkey: Studies of the interlaminar zones and the S layers. J Comp Neurol 213:135–145
Weller RE, Kaas JH (1989) Parameters affecting the loss of ganglion cells of the retina following ablations of striate cortex in primates. Vis Neurosci 3:327–349
Weiskrantz L (1989) Blindsight. In: Boller F, Grafman J (eds) Handbook of neuropsychology, Vol 2, Elsevier, Amsterdam, pp 375–385
Wilson JR (1989) Synaptic organization of individual neurons in the macaque lateral geniculate nucleus. J Neurosci 9:2931–2953
Wilson JR, Hendrickson AE (1981) Neuronal and synaptic structure of the dorsal lateral geniculate nucleus in normal and monocularly deprived macaca monkeys. J Comp Neurol 197:517–539
Yu BC-Y, Watt CB, Lam DMK, Fry KR (1988) GABAergic ganglion cells in the rabbit retina. Brain Res 439:376–382
Yukie M, Iwai E (1981) Direct projection from dorsal lateral geniculate nucleus to the prestriate cortex in macaque monkeys. J Comp Neurol 201:81–97